

Contributions to the Selection of Solvents in the Extraction of Phenolic Acids

Rebeca Silva Alves

Dissertation presented to

**Escola Superior de Tecnologia e Gestão
Instituto Politécnico de Bragança**

In order to obtain Master's Degree in

Chemical Engineering

This work was supervised by

Maria Olga Amorim e Sá Ferreira

Simão Pedro Almeida Pinho

Leila Maria Aguilera Campos

February, 2019

“When you lose small mind, you free your life.”

System of a Down

Acknowledgments

I would like to give a special thanks to my supervisors from IPB, professors Simão Pinho and Olga Ferreira, for all their dedication, encouragement, concern, guidance, patience and all the learning during this year.

I also would like to thank the professors from UNIFACS, Leila Campos, Diniz Silva, Ronaldo Costa and Luiz Pontes for their support and encouragement to come to Portugal, especially to professor Leila for the years of guidance and learning.

I cannot let to thank all the friends I have made during this year, especially to Sérgio Vilas Boas, for teamwork, for your patience and support. Work is much easier when we feel good and welcomed.

I am immensely grateful to my family for education, support, attention and love, especially to my parents Eloina and Renaldo, without them I would not be who I am.

I also thank the International Office, for giving me the opportunity to attend the Double Degree Program formed by the partnership of UNIFACS and IPB.

To everyone who contributed directly or indirectly to this dissertation, my sincere thanks!

This work is a result of: Project “AIProcMat@N2020 - Advanced Industrial Processes and Materials for a Sustainable Northern Region of Portugal 2020”, with the reference NORTE-01-0145-FEDER-000006, supported by Norte Portugal Regional Operational Programme (NORTE 2020), under the Portugal 2020 Partnership Agreement, through the European Regional Development Fund (ERDF); Associate Laboratory LSRE-LCM - UID/EQU/50020/2019 - funded by national funds through FCT/MCTES (PIDDAC); Project AllNat - POCI-01-0145-FEDER-030463, financed by COMPETE and Portugal2020 and national funds through FCT.

Abstract

Naturally occurring phenolic acids are well-known and studied for their bioactive properties and wide distribution in plants, where they can be found in free form, or conjugated to other molecules. The study of the solubility of phenolic compounds in water and organic solvents is thus fundamental for the design of extraction, separation, crystallization and purification processes of great importance in the pharmaceutical, cosmetics and food industries.

In this context, the main objective of this work is to measure the solubility of *trans*-cinnamic, *p*-coumaric and ferulic acids in water and in seven organic solvents (methanol, ethanol, 1-propanol, 2-propanol, 2-butanone, ethyl acetate and acetonitrile) at 298.2 K and 313.2 K and test the ability of the NRTL-SAC model, with or without the Reference Solvent Approach (RSA), and the Abraham solvation model to correlate, and preferably, predict the solubility data.

To accomplish the objectives above the shake-flask method experimental method was combined with UV-Visible spectroscopy and gravimetric methods of analysis to perform the solubility measurements. In general, the results obtained were in close agreement with the very scarce information available in literature.

After, the NRTL-SAC segment descriptors of each solute were fitted to solubility data in seven solvents, obtaining average relative errors (ARD) between 23% and 39%. The model was then applied to predict the solubility in other eight solvents, with ARD between 42% and 61%. The RSA was also applied, but no significant improvements were obtained relatively to the first approach. The optimization parameters of the Abraham solutes were also obtained by fitting the solubility data in six solvents for the *trans*-cinnamic and *p*-coumaric acids, and seven solvents for the ferulic acid, obtaining ARD between 7% and 24% for correlations and between 4% and 33% for the predictions in the remaining solvents. These values indicate Abraham's solvation model as the most suitable and very satisfactory model to predict the solubility of the selected solutes at 298.2 K.

Keywords: solubility, phenolic compounds, NRTL-SAC model, Abraham solvation model

Resumo

Os ácidos fenólicos de ocorrência natural são bem conhecidos e estudados por suas propriedades bioativas e ampla distribuição em plantas, onde podem ser encontrados na forma livre ou conjugados com outras moléculas. O estudo da solubilidade de compostos fenólicos em água e solventes orgânicos é fundamental para a concepção de seus processos de extração, separação, cristalização e purificação de grande importância nas indústrias farmacêutica, cosmética e alimentar.

Nesse contexto, o principal objetivo deste trabalho é a medição de solubilidade dos ácidos *trans*-cinâmico, *p*-cumárico e ferúlico em água, e em diferentes solventes orgânicos (metanol, etanol, 1-propanol, 2-propanol, 2-butanona, acetato de etilo e acetonitrilo) a 298,2 K e 313,2 K e testar a capacidade dos modelos NRTL-SAC, combinado ou não com a metodologia do Solvente Referência (RSA), e do modelo de solvatação de Abraham para correlacionar e, preferencialmente prever, os dados de solubilidade.

Para atingir esses objetivos, o método dos frascos agitados, combinado com os métodos de espectroscopia de UV-Visível e o gravimétrico, foram selecionados para efetuar as medições de solubilidade. Em geral, os resultados obtidos são bem consistentes com as escassas informações disponíveis na literatura.

Finalmente, os descritores de segmentos do soluto NRTL-SAC foram obtidos através do ajuste de dados de solubilidade em sete solventes, obtendo-se um erro relativo médio (ARD) entre 23% e 39%. O modelo foi então avaliado quanto à sua capacidade para prever a solubilidade em oito solventes, obtendo-se um ARD entre 42% e 61%. Os parâmetros dos solutos no modelo de Abraham foram obtidos através do ajuste de dados de solubilidade em seis solventes para os ácidos *trans*-cinâmico e *p*-cumárico, e sete solventes para o ácido ferúlico, obtendo-se um ARD entre 7% e 24% para as correlações e entre 4% e 33% para as previsões em sete solventes. Esses valores indicam o modelo de solvatação de Abraham como o mais promissor para prever a solubilidade dos solutos estudados a 298,2 K.

Palavras-chave: solubilidade, compostos fenólicos, modelo NRTL-SAC, modelo de solvatação de Abraham

Table of Contents

List of Symbols and Acronyms	xi
List of Tables	xiii
List of Figures.....	xv
Chapter 1. Introduction	1
1.1. Framework and Objectives	1
1.2. Contents	2
Chapter 2. State of Art	3
2.1. Phenolic Compounds	3
2.1.1. <i>Trans</i> -Cinnamic Acid.....	4
2.1.2. <i>p</i> -Coumaric Acid.....	4
2.1.3. Ferulic Acid	4
2.2. Solid-Liquid Equilibria	5
2.2.1. Melting Properties.....	5
2.2.2. Solubility Measurements.....	6
2.3. Thermodynamic Modelling.....	8
2.3.1. Non-Random Two-Liquid Segment Activity Coefficient Model (NRTL-SAC)	9
2.3.3. The Abraham Solvation Model.....	10
Chapter 3. Experimental work	12
3.1. Materials	12
3.2. Methods.....	12
3.2.1. Differential Scanning Calorimetry	12
3.2.2. Solubility Experimental Method	13
3.3. Results and Discussion	15
3.3.1. Melting Properties.....	15
3.3.2. Solubility Measurements.....	16
Chapter 4. Thermodynamic Modeling.....	25

4.1. The NRTL-SAC Model	25
4.2. The Abraham Solvation Model.....	30
Chapter 5. Conclusions and Future Work	33
References	35
Appendix A: Literature Solubility Data of <i>t</i> -CA, <i>p</i> -CA and FA.....	40
Appendix B: NRTL-SAC Parameters from Literature	45
Appendix C: Abraham’s Solvation Model Coefficients from Literature	48
Appendix D: Calibration Curves by UV-Vis Spectroscopy	50
Appendix E: Results from Differential Scanning Calorimetry.....	52

List of Symbols and Acronyms

List of Symbols

$\log P$	Partition Coefficient
M	Molar Mass (g/mol)
R	Ideal Gas Constant
S	Mass Fraction Solubility
x	Mole Fraction Solubility
Γ_m	Segment Activity Coefficient
r_I	Total Segment Number of Species I
ϕ_I	Segment Mole Fraction of Species I
T	Absolute Temperature (K)
T_m	Melting Point Temperature (K)
γ_I	Activity Coefficient of Species I
$\Delta_m H$	Melting Enthalpy (kJ/mol)

List of Acronyms

ARD (%)	Average Relative Deviation (%)
CAS	Chemical Abstracts Number
DSC	Differential Scanning Calorimetry
DMSO	Dimethyl Sulfoxide
CPA-EoS	Cubic-Plus-Association Equation of State
FA	Ferulic Acid
HPLC	High-Performance Liquid Chromatography

LFER	Linear Free Energy Relationships
NRTL-SAC	Nonrandom Two-Liquid Segment Activity Coefficient
<i>p</i> -CA	<i>p</i> -Coumaric Acid
PR-EoS	Peng-Robinson Equation of State
RSA	Reference Solvent Approach
<i>t</i> -CA	<i>trans</i> -Cinnamic Acid
UNIQUAC	Universal Quasichemical Model
UV-Vis	Ultraviolet Visible Radiation

List of Tables

Table 2.1 Overview of the literature melting temperature and enthalpy of the compounds studied in this work.	6
Table 2.2 Literature overview of solubility data of the cinnamic acids in water and organic solvents, studied in this work, and the corresponding experimental methodologies.	7
Table 2.3 Thermodynamic models applied to describe the solubility of the compounds studied in this work.	8
Table 3.1 Mass purity (%) and supplier of the organic compounds used in this work.	12
Table 3.2 Wavelengths used for UV-Vis spectrophotometry measurements.	15
Table 3.3 Comparison between the melting properties measured in this work and the average literature values.	16
Table 3.4 Solubility (g of solute per 100 g of solvent) of the studied cinnamic acids at 298.2 K in water and organic solvents measured by UV-Vis spectroscopy.	16
Table 3.5 Solubility (g of solute per 100 g of solvent) of the studied cinnamic acids at 313.2 K in water and organic solvents measured by UV-Vis spectroscopy.	17
Table 3.6 Solubility (g of solute per 100 g of solvent) of the studied cinnamic acids in water and organic solvents at 298.2 K measured by gravimetry.	17
Table 3.7 Solubility (g of solute per 100 g of solvent) of the studied cinnamic acids in water and selected organic solvents at 313.2 K measured by gravimetry.	18
Table 4.1 NRTL-SAC optimized parameters and ARD (%) for each cinnamic acid using water and six organic solvents in the fitting.	26
Table 4.2 ARD (%) and experimental data (<i>NP</i>) for each solvent used in simulation.	26
Table 4.3 NRTL-SAC + RSA approach optimized parameters and ARD (%) for each cinnamic acid using water and six organic solvents in the fitting.	28
Table 4.4 ARD (%) and number of experimental data (<i>NP</i>) for each solvent used in simulation.	29
Table 4.5 Density at 25°C and refractive index of the cinnamic acids studied in this work.	30
Table 4.6 Abraham estimated solute's parameters and ARD (%) for each hydroxycinnamic acid using water and six organic solvents in the fitting.	30
Table 4.7 Abraham optimized solute's parameters and ARD (%) for ferulic acid using water and seven organic (including DMSO) solvents in the fitting.	31

Table 4.8 ARD (%) and number of points (<i>NP</i>) for each solvent used in simulation (second optimization round for ferulic acid).....	31
Table A.1 Solubility in mole fraction of <i>trans</i> -cinnamic acid in organic solvents measured by Li <i>et al.</i> (2016).....	40
Table A.2 Solubility in g/L of <i>trans</i> -cinnamic acid in water.	40
Table A.3 Solubility (g of solute per 100 g of solvent) of <i>trans</i> -cinnamic acid in methanol and ethanol, measured by Soares (2017).....	40
Table A.4 Solubility in mole fraction of <i>p</i> -coumaric acid in ethyl acetate.	41
Table A.5 Solubility in mole fraction of <i>p</i> -coumaric acid in organic solvents measured by Ji <i>et al.</i> (2016).	41
Table A.6 Solubility in mole fraction of ferulic acid in organic solvents.	42
Table A.7 Solubility in mole fraction of ferulic acid in water.	43
Table A.8 Solubility in mol/kg of ferulic acid in water measured by Noubigh <i>et al.</i> (2007).....	43
Table A.9 Solubility in g/L of ferulic acid in water measured by Mota <i>et al.</i> (2008).....	44
Table A.10 Solubility in mole fraction of cinnamic acids in solvents not studied in this work.....	44
Table B.1 NRTL Binary parameters for conceptual segments in NRTL-SAC (Chen and Song, 2004). ...	45
Table B.2 NRTL-SAC molecular parameters for common solvents (Chen and Crafts, 2006).....	45
Table C.1 Coefficients in the linear free energy relationships (LFER) for water–solvent partitions as log <i>P</i> at 25 °C (Abraham <i>et al.</i> , 2015), considering dry solvents.....	48

List of Figures

Figure 2.1 Crystal and chemical structures of the cinnamic acids studied in this work: (a) <i>trans</i> -cinnamic acid; (b) <i>p</i> -coumaric acid and (c) <i>trans</i> -ferulic acid.....	3
Figure 3.1 Solubility of <i>trans</i> -cinnamic acid in water as a function of stirring time. The line is a guide for the eyes.	14
Figure 3.2 Solubility of the cinnamic acids in water and organic solvents measured by UV-Vis spectroscopy at (a) 298.2 K and (b) 313.2 K.	19
Figure 3.3 Solubility of <i>trans</i> -cinnamic acid in water and organic solvents (a) water, (b) ethanol, (c) methanol, (d) 1-propanol and (e) 2-propanol as function of temperature: (■) (Li <i>et al.</i> , 2016), (●) (Soares, 2017), (▲) (Mota <i>et al.</i> , 2008) and (★) this work.....	20
Figure 3.4 Solubility of <i>p</i> -coumaric acid in water and organic solvents (a) ethanol, (b) methanol, (c) 1-propanol, (d) 2-propanol and (e) ethyl acetate as function of temperature:, (◀) (Ji <i>et al.</i> , 2016), (▼) (Alevizou and Voutsas, 2013) and (★) this work.	22
Figure 3.5 Solubility of ferulic acid in water and organic solvents (a) water, (b) ethanol, (c) methanol, (d) 2-propanol and (e) ethyl acetate as function of temperature: (◆) (Bitencourt <i>et al.</i> , 2016), (●) (Shakeel <i>et al.</i> , 2017), (▶) (Noubigh <i>et al.</i> , 2007), (◆) (Haq <i>et al.</i> , 2017), (▲) (Mota <i>et al.</i> , 2008) and (★) this work.	23
Figure 4.1 Comparison between experimental and calculated solubility using the NRTL-SAC model: (a) correlation; (b) prediction.	27
Figure 4.2 Comparison between experimental and calculated solubility using the NRTL-SAC model combined with the RSA: (a) correlation; (b) prediction.	29
Figure 4.3 Comparison between experimental and calculated solubility using the Abraham solvation model: (a) correlation results; (b) predictions.	32
Figure D.1 Calibration curve of <i>trans</i> -cinnamic acid in water + ethanol (35:65, wt.%) mixed solvent, at 273 nm.	50
Figure D.2 Calibration curve of ferulic acid in water + ethanol (35:65, wt.%) mixed solvent, at 321 nm.	50
Figure D.3 Calibration curve of <i>p</i> -coumaric acid in water + ethanol (35:65, wt.%) mixed solvent, at 310 nm.	51
Figure E.1 Differential scanning calorimetry diagram of <i>trans</i> -cinnamic acid.	52

Figure E.2 Differential scanning calorimetry diagram of ferulic acid.....	52
Figure E.3 Differential scanning calorimetry diagram of <i>p</i> -coumaric acid.	53

Chapter 1. Introduction

1.1. Framework and Objectives

The study of the solubility of phenolic compounds in water, organic solvents and, more recently, alternative solvents such as ionic liquids and eutectic solvents, is fundamental for the design of their separation processes in the pharmaceutical, cosmetic and food industries.

Particularly, the solubility has a great relevance in the pharmaceutical industry, both in the discovery and development phases of drug research, as well as for biopharmaceutical classification and bioequivalence issues. To perform those tests and optimize the drugs formulation, a large amount of water solubility data are required because this property is directly related to the pharmacokinetic properties of a drug and therefore its effects in human organism (Baka *et al.*, 2008; Martins *et al.*, 2013).

The solubility of an organic compound is directly related to the molecular structure and the specific interactions involving both the solute and the solvent. The solubility of solids or liquids in another liquid will only occur if the interaction between the solute and the solvent is sufficiently high to promote the rupture of solute-solute and solvent-solvent interactions. Thus, polar solutes tend to dissolve better in polar solvents, whereas nonpolar, or weakly polar substances, are more likely to be dissolved in nonpolar systems (Martins *et al.*, 2013).

In our research group, previous studies were focused on the solubility of some natural phenolic compounds in water (Mota *et al.*, 2008), the solubility of flavonoids in pure organic solvents (Ferreira and Pinho, 2012) or mixed solvents (Ferreira *et al.*, 2013), the solubility of poorly soluble compounds in water and mixed solvents (Soares, 2017) and the solubility of hydroxybenzoic acids in water and organic solvents (Vilas-Boas, 2017). Following those previous works, the main objective of this master dissertation is the measurement of the solubility of naturally occurring cinnamic acids such as ferulic acid, *p*-coumaric acid and *trans*-cinnamic acid in water and organic solvents, considering solvents of diverse polarity, hydrophobicity and

functionality. Furthermore, the experimental data will be described using the non-random two-liquid segment activity coefficient (NRTL-SAC) model and the Abraham solvation model, aiming to predict, at least qualitatively, the order of magnitude of the solubility.

1.2. Contents

Chapter 2 starts with a description of the chemical and biological properties of the phenolic compounds selected in this work, considering also their applications. The most common experimental methods for measuring the solubility of solids in liquids is also described. In addition, a literature review focusing on the measurements of the melting properties and solubility of the three compounds evaluated in this work was conducted. This chapter finishes by presenting the main thermodynamic models commonly used to describe the solid-liquid equilibria of the compounds studied here, with particular emphasis on the NRTL-SAC model combined or not with the Reference Solvent Approach (RSA), and the Abraham's solvation model.

The experimental part of this work is described in Chapter 3, including the materials, methods and the results obtained regarding the melting properties and the solubilities of the studied acids. Chapter 4 is dedicated to the thermodynamic modeling of the solubility results. Finally, in Chapter 5, the main conclusions and some suggestions for future work are summarized.

Chapter 2. State of Art

2.1. Phenolic Compounds

Phenolic compounds are a diverse group of aromatic secondary plant metabolites. They are widely distributed, in both edible and non-edible plants, as esters or glycoside derivatives, and are synthesized by plants during their development. By definition, they have a common structural feature: an aromatic ring bonded to at least one hydroxyl substituent. These compounds play an important role in growth and reproduction, providing protection against pathogens and predators (Bravo, 1998; Stalikas, 2007; Dávalos *et al.*, 2012).

The class of hydroxycinnamic acids is formed by an aliphatic group and a carboxylic acid group, in addition to the aromatic ring. In this work, two phenolic acids were selected from the class of hydroxycinnamic acids: *p*-coumaric acid and ferulic acid. The number and positions of the hydroxyl or methoxy groups on the aromatic ring distinguishes the latter compounds, as can be seen in Figure 2.1. For comparison purposes, *trans*-cinnamic acid was also studied as they are derived from it.

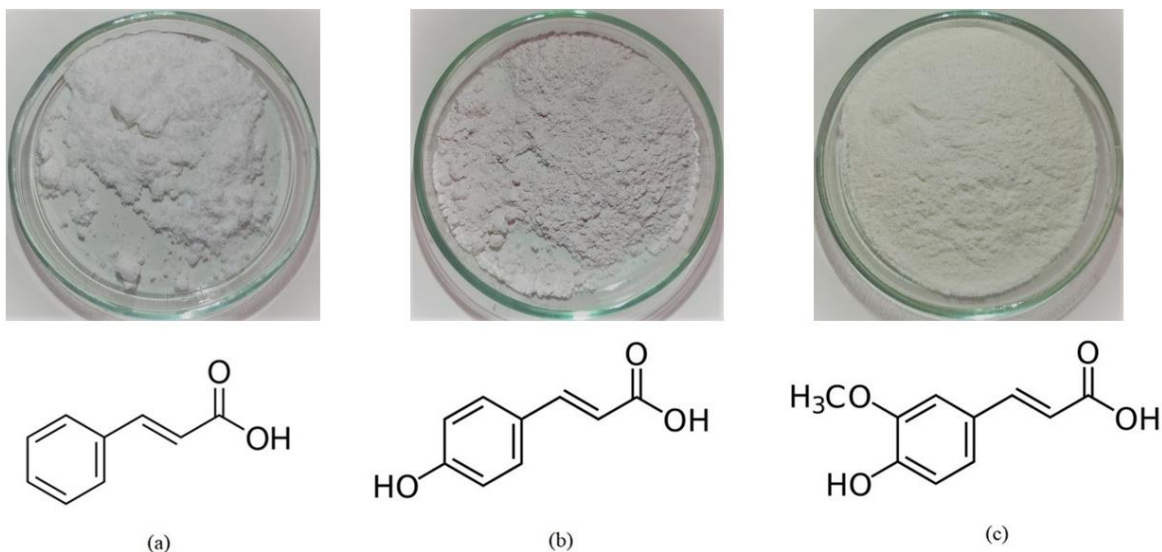


Figure 2.1 Crystal and chemical structures of the cinnamic acids studied in this work: (a) *trans*-cinnamic acid; (b) *p*-coumaric acid and (c) *trans*-ferulic acid.

2.1.1. *Trans*-Cinnamic Acid

Trans-cinnamic acid (*t*-CA, C₉H₈O₂) is the predominant form of natural cinnamic acid. It is a white oily phenolic powder, present in some dietary plants, fruits, and herbs. It can be used as a preservative for grain, fruits, and vegetables and as a raw material in the organic synthesis, with applications in the pharmaceutical and agricultural industries. In addition, *trans*-cinnamic acid presents potential antibacterial, anti-inflammatory, antifungal, antitumor activities and therapeutic effects in cardiovascular diseases due to its antioxidant properties (Wang *et al.*, 2015).

In the pharmaceutical and food industries, for example, *trans*-cinnamic acid has been studied as a potential inhibitor to blockade invasion and metastasis for a wide range of tumors (Jia *et al.*, 2008) and it is the main raw material in the production of L-phenylalanine, one of the two precursors required for the synthesis of artificial sweetener aspartame (Yen *et al.*, 2011).

2.1.2. *p*-Coumaric Acid

Coumaric acid is a nutraceutical and phytochemical compound that exists in three isomers (ortho-, meta-, and para-), with *p*-coumaric acid being the most abundant in nature. *p*-Coumaric acid (*p*-CA, C₉H₈O₃) is a yellowish purple crystalline powder found in *diffusa*, *bodhisattva*, *eucommia*, peanuts, red wine, tea, apples, beans, and tomatoes. It can be found in plants in the free form, or conjugated to other molecules, such as amines, organic acids, alcohols, mono- or oligosaccharides, and lignin (Bevill *et al.*, 2014; Ferreira *et al.*, 2018).

p-Coumaric acid exhibits antioxidant, anti-inflammatory, and antiangiogenic properties with possible application in the prevention of type 2 diabetes, anti-cancer activity in human cancer cells by suppression of metastatic and angiogenic potential, preventing cataract formation and treatment of cosmetic imperfections (Papadopoulos and Boskou, 1991; Bevill *et al.*, 2014; Kim *et al.*, 2016; Peng *et al.*, 2018).

2.1.3. Ferulic Acid

Ferulic acid (FA, C₁₀H₁₀O₄), a white to off-white crystalline solid, is a highly abundant phenolic phytochemical present in the plant cell walls, and it is found in vegetables and fruits, and in seeds of plants such as brown rice, whole wheat, and oats, as well as in wine, olive oil, coffee, apple, artichoke, peanut, orange, and pineapple. It is a phenolic compound which has various

applications in biomedical, pharmaceutical and food industries (Bitencourt *et al.*, 2016; Haq *et al.*, 2017).

A review by Ou and Kwok (2004) shows the diverse applications of ferulic acid in the pharmaceutical and food industries. As pharmaceutical functions are emphasized the anti-oxidant, cholesterol-lowering, antimicrobial and anti-inflammatory activities, the prevention against thrombosis and atherosclerosis. As applications in foods, it is used in the production of vanillin, an important aromatic flavor compound, as an ingredient in sport foods and skin lotions, as well as a preservative because of its antioxidant and antimicrobial activities.

More recent studies emphasize the antioxidant properties of ferulic acid and its anticancer potential, for example, in hepatocellular cancer inhibition, the most common type of malignant hepatoma cancer (Mathew and Abraham, 2004; Pacheco-Palencia *et al.*, 2008; Cheng *et al.*, 2018; Preedia Babu *et al.*, 2018).

2.2. Solid-Liquid Equilibria

In this section, a literature review is presented regarding the experimental methods to measure the melting properties by DSC and the solubility, as well as a database containing the solid-liquid equilibria data of the three selected compounds (*trans*-cinnamic acid, *p*-coumaric acid and ferulic acid).

2.2.1. Melting Properties

Table 2.1 presents an overview of the melting properties available in literature. As can be seen, the information was mainly obtained by DSC with heating rates varying between 1 K·min⁻¹ and 10 K·min⁻¹.

In general, the melting temperatures (T_m) of the cinnamic acids are consistent among different authors; however, significant variations in the melting enthalpies ($\Delta_m H$) can be observed. For example, Alevizou and Voutsas (2013) and Ji *et al.* (2016) used the same methodology to measure $\Delta_m H$ of *p*-coumaric acid, but they reported divergent values, 27.42 kJ·mol⁻¹ and 34.30 kJ·mol⁻¹, respectively.

Table 2.1 Overview of the literature melting temperature and enthalpy of the compounds studied in this work.

Compound	T_m (K)	$\Delta_m H$ (kJ·mol ⁻¹)	Methodology	Reference
<i>trans</i> -cinnamic acid	406.15	22.63	NA ^a	(Acree, 1991)
	406.10 ± 0.40	22.21 ± 0.82	DSC 1 K·min ⁻¹ heating rate	(Mota <i>et al.</i> , 2008)
	404.80	22.64	DTG ^b /DSC	(Sharma <i>et al.</i> , 2004)
	406.15 ± 0.30	22.21 ± 0.36	DSC 10 K·min ⁻¹ heating rate	(Li <i>et al.</i> , 2016)
<i>p</i> -coumaric acid	492.35 ± 0.30	27.42 ± 0.90	DSC 10 K·min ⁻¹ heating rate	(Alevizou and Voutsas, 2013)
	494.35 ± 0.20	34.30	DSC 10 K·min ⁻¹ heating rate	(Ji <i>et al.</i> , 2016)
ferulic acid	445.1 ± 0.9	33.5 ± 0.5	DSC 10.2 K·s ⁻¹ heating rate	(Dávalos <i>et al.</i> , 2012)
	444.60 ± 0.51	33.34 ± 1.23	DSC 1 K·min ⁻¹ heating rate	(Mota <i>et al.</i> , 2008)
	445.9	34.7	DSC 10 K·min ⁻¹ heating rate	(Emel'yanenko <i>et al.</i> , 2016)
	444.9 ± 0.4	31.9 ± 0.9	DSC 3 K·min ⁻¹ heating rate	(Manic <i>et al.</i> , 2012)
	447.70	36.27	DSC 10 K·min ⁻¹ heating rate	(Shakeel <i>et al.</i> , 2017)

^aNot available. ^bDifferential thermogravimetry.

2.2.2. Solubility Measurements

Solubility measurements can be performed by direct and indirect methods. In direct methods, the solubility is measured from chemical analysis of the phases in equilibrium, known as analytical methods, or by varying the properties (temperature, pressure, composition, etc.) of a saturated solution of known mass, called synthetic methods (Hefter and Tomkins, 2003). In indirect methods, the solubility product is determined before the solubility is measured.

In order to evaluate the most adequate experimental methodology to perform the solubility measurements, as well as to evaluate the amount of available solubility data of the compounds studied in this work, a literature review is compiled in Table 2.2. The gathered data is presented in more detail in Tables A.1 to A.9 for solvents studied in this work (Appendix A).

Table 2.2 Literature overview of solubility data of the cinnamic acids in water and organic solvents, studied in this work, and the corresponding experimental methodologies.

Solute	Solvent	Temperature range (K)	Experimental methodology	Shaking time (h)	Settling time (h)	Reference
<i>trans</i> -cinnamic acid	methanol, ethanol, isopropyl alcohol, and propanol	283 – 333	last crystal disappearance	2	-	(Li <i>et al.</i> , 2016)
	water, ethanol, and methanol	298	shake-flask coupled to gravimetric and spectrophotometric methods	30	12	(Soares, 2017)
<i>trans</i> -cinnamic acid and ferulic acid	water	288 – 323	shake-flask coupled to gravimetric and spectrophotometric methods	64 - 156	6 - 75	(Mota <i>et al.</i> , 2008)
ferulic acid	water	293 – 318	shake-flask coupled to HPLC	3	3	(Noubigh <i>et al.</i> , 2007)
	ethanol and water	293 – 333	shake-flask coupled to gravimetric method	1	24	(Bitencourt <i>et al.</i> , 2016)
	isopropanol and water	298 – 318	shake-flask coupled to HPLC and UV-Vis (322 nm)	72	24	(Haq <i>et al.</i> , 2017)
	water, methanol, ethanol, isopropanol, and ethyl acetate	298 – 318	shake-flask coupled to reversed phase-HPLC and UV-Vis (322 nm)	72	24	(Shakeel <i>et al.</i> , 2017)
<i>p</i> -coumaric acid	ethyl acetate	303 – 317	saturation method in a Thermomixer Comfort (1400 rpm) coupled to HPLC and UV-Vis (320 nm)	24 - 192	-	(Alevizou and Voutsas, 2013)
	methanol, ethanol, 1-propanol, 2-propanol, and ethyl acetate	293 – 333	shake-flask coupled to gravimetric method	72	12	(Ji <i>et al.</i> , 2016)

2.3. Thermodynamic Modelling

Besides measuring solubility data as a function of temperature, being these data fundamental for designing industrial processes, due to the long time for measurements and the unavailability of reagents, it is also fundamental to apply thermodynamic models to correlate and predict the solubility of a compound in different solvents and process conditions. In Table 2.3, a review of the thermodynamic models used to describe the solubility data presented in Table 2.2 is summarized.

Table 2.3 Thermodynamic models applied to describe the solubility of the compounds studied in this work.

Solute	Solvent	Models	Reference
<i>trans</i> -cinnamic acid	methanol, ethanol, isopropyl alcohol, and propanol	Apelblat, λ h, NRTL and UNIQUAC	(Li <i>et al.</i> , 2016)
<i>trans</i> -cinnamic acid and ferulic acid	water	CPA-EoS	(Mota <i>et al.</i> , 2008)
<i>p</i> -coumaric acid	ethyl acetate	UNIQUAC and NRTL	(Alevizou and Voutsas, 2013)
	methanol, ethanol, 1-propanol, 2-propanol, and ethyl acetate	Apelblat, λ h, NRTL, UNIQUAC and Wilson for pure solvents; Apelblat and Jouyban-Acree for the mixed solvents	(Ji <i>et al.</i> , 2016)
ferulic acid	water	No model was applied	(Noubigh <i>et al.</i> , 2007)
	ethanol and water	PR- EoS	(Bitencourt <i>et al.</i> , 2016)
	isopropanol and water	Apelblat, Yalkowsky and Jouyban-Acree models	(Haq <i>et al.</i> , 2017)
	water, methanol, ethanol, isopropanol, and ethyl acetate	Apelblat model	(Shakeel <i>et al.</i> , 2017)

As can be seen, in general, classical activity coefficient models such as Apelblat, NRTL, UNIQUAC or Wilson models have been applied. Two equations of state were also tested: the cubic-plus-association equation of state (CPA-EoS) and the Peng-Robinson equation of state (PR-EoS). However, these models have a predictive capacity that is limited by the use of molecular interaction parameters. In the following sections, hybrid models with much higher prediction potentialities are being presented.

2.3.1. Non-Random Two-Liquid Segment Activity Coefficient Model (NRTL-SAC)

The non-random two-liquid segment activity coefficient thermodynamic model (NRTL-SAC), a derivative of the original NRTL model of Renon and Prausnitz (1968), was proposed by Chen and Song (2004). The model has two main terms, that are the combinatorial (C) and the residual (R) contributions to the activity coefficient of component I (γ_I):

$$\ln \gamma_I = \ln \gamma_I^C + \ln \gamma_I^R \quad (1)$$

The residual contribution is calculated from the local composition (lc) interaction of the polymer NRTL model:

$$\ln \gamma_I^R = \ln \gamma_I^{lc} = \sum_m r_{m,I} [\ln \Gamma_m^{lc} - \ln \Gamma_m^{lc,I}] \quad (2)$$

Then, the segment activity coefficient Γ_m can be calculated from the NRTL equation. The combinatorial term is based on the Flory-Huggins term, as follows:

$$\ln \gamma_I^C = \ln \frac{\phi_I}{x_I} + 1 - r_I \sum_J \frac{\phi_J}{r_J} \quad (3)$$

$$r_I = \sum_i r_{i,I} \quad (4)$$

$$\phi_I = \frac{r_I x_I}{\sum_J r_J x_J} \quad (5)$$

where r_I and ϕ_I are the total segment number and segment mole fraction of component I , respectively.

NRTL-SAC describes each component using four types of conceptual segments related to the different surface interactions: hydrophobicity (X), hydrophilicity (Z), polarity ($Y+$), and solvation strength ($Y-$) (Chen *et al.*, 2008). Chen and Song (2004) and Chen and Crafts (2006) already reported the segment descriptors of 62 common solvents commonly used in the pharmaceutical industry, which are presented in Tables B.1 and B.2 (Appendix B). Therefore, a small set of experimental solubility data is usually used to estimate the four segment parameters missing for each solute.

Assuming pure solid phase and neglecting the heat capacity difference upon melting, classical thermodynamics proposes equation 6 to describe the solubility curves:

$$\ln x_S \gamma_S = \frac{\Delta_m H}{RT_m} \left(1 - \frac{T_m}{T}\right) \quad (6)$$

where x_S is the mole fraction of solute S , γ_S is the activity coefficient of solute S , $\Delta_m H$ its melting enthalpy, R is the ideal gas constant, T_m is the melting temperature of the solute, and T is the absolute temperature.

To avoid the use of thermal properties, often unknown or unreliable for the studied compounds, a second approach is proposed in which the NRTL-SAC model is combined with the reference solvent approach (RSA) (Abildskov and O'Connell, 2005). This methodology can be represented by the following equation:

$$\ln x_{Si} = \ln x_{Sj} + \ln \gamma_{Sj}(T, \{x_S\}_j) - \ln \gamma_{Si}(T, \{x_S\}_i) \quad (7)$$

where x_{Si} is the mole fraction solubility of solute S in solvent i , x_{Sj} is the mole fraction solubility of S in reference solvent j , $\gamma_{Si}(T, \{x_S\}_i)$ is the activity coefficient of S in solvent i , while $\gamma_{Sj}(T, \{x_S\}_j)$ is the activity coefficient of S in the reference solvent j .

The optimal reference solvent j is found by minimizing the sum of the residuals according to equation (8):

$$\min_j |\sum_{i=data} \delta \ln x_{S,ij}| = \min_j |\sum_{i=data} (\ln x_{Si} + \ln \gamma_{Si}) - N(\ln x_{Sj} + \ln \gamma_{Sj})| \quad (8)$$

being $x_{S,ij}$ the mole fraction of component S in solvent i , assuming that j is the reference solvent, and, finally, N is the number of experimental data.

2.3.3. The Abraham Solvation Model

The Abraham solvation model was proposed by Abraham *et al.* (2004). The method is based on the assumption that the partition between water and a solvent, P_s , is given by the ratio of solubilities of a solute in the solvent, S_s , and in water, S_w :

$$P_s = \frac{S_s}{S_w} \quad (9)$$

The partition coefficients between water and a large number of phases can be predicted through a series of linear free energy equations (LFER), so that if S_w is known, then S_s can be

predicted and, in cases where S_w is unknown, it can be estimated if solubilities in other solvents are available. Equation 10 is used to obtain the partition coefficients between two liquid phases:

$$\log P_s = c + eE + sS + aA + bB + vV \quad (10)$$

where the parameters in lowercase letters refer to the solvent and are available in Appendix C. The independent variables in capital letters refer to the solute: E is the solute excess molar refractivity, S is the solute dipolarity/polarizability, A and B are the overall or summation hydrogen bond acidity and basicity, respectively, and V is the McGowan characteristic volume. Part or all of those coefficients can be obtained by multiple linear regression analysis and serve to characterize a solute. V is calculated from the molecular formula of the solute and the number of bonds (N_B) in the molecule from the following equation:

$$N_B = N_A - 1 + N_R \quad (11)$$

where N_A is the total number of atoms and N_R is the number of rings.

As the solutes studied in this work are solids, E can be estimated using the ACD software (ACD/ChemSketch, Advanced Chemistry Development Inc., 2017.1.2 version). To estimate the three independent parameters that are missing (A , B and S), if experimental $\log P_s$ values are measured or available in the literature, the parameters can be obtained using simply the "Solver" add-on in Microsoft Excel.

Chapter 3. Experimental work

3.1. Materials

All the compounds were used as received, and the solids kept in a desiccator to avoid water contamination. Ultrapure water (resistivity of 18.2 M Ω ·cm, free particles \geq 0.22 μ m and total organic carbon < 5 μ d·dm⁻³) was used to perform the solubility experiments. The mass purity and source of all the compounds used in this work are listed in Table 3.1.

Table 3.1 Mass purity (%) and supplier of the organic compounds used in this work.

Component	Mass Purity (%)	CAS number	Source
<i>trans</i> -cinnamic acid	\geq 99.5	140-10-3	Alfa Aesar
<i>p</i> -coumaric acid	\geq 99.9	7400-08-0	Merck KGaA
<i>trans</i> -ferulic acid	\geq 99.9	537-73-5	Alfa Aesar
methanol	\geq 99.9	67-56-1	Carlo Erba
ethanol	\geq 99.9	64-17-5	Carlo Erba
2-propanol	\geq 99.9	67-63-0	Honeywell
1-propanol	\geq 99.5	71-23-8	Carlo Erba
2-butanone	\geq 99.5	78-93-3	Sigma Aldrich
ethyl acetate	\geq 99.9	141-78-6	Carlo Erba
acetonitrile	\geq 99.9	75-05-8	Sigma Aldrich

3.2. Methods

3.2.1. Differential Scanning Calorimetry

The melting properties were measured by Differential Scanning Calorimetry (DSC). For this, the DSC TG 209 F3 Tarsus of Netzsch was calibrated with benzoic acid, indium, caffeine, bismuth, 4-nitroluene, water, naphthalene, diphenylacetic acid, anthracene, tin, and zinc at the onset temperature, ensuring a reliability within 1.53% in the temperature range from 0 °C to

420 °C. For DSC analysis, the temperature ranged from 20 °C to the melting point temperature, with a heating rate of 1 K·min⁻¹, under nitrogen flow. For each acid, at least three runs were performed.

3.2.2. Solubility Experimental Method

In this work, a direct analytical method was applied. The shake-flask technique is based on the preparation of a saturated solution of the system studied. The equilibrium is achieved by magnetic stirring, and the time for it to occur may vary depending on the properties of the sample and the equilibrium method used. After reaching equilibrium, the undissolved excess solid is settled down during a given time. When the equilibrium is achieved, a sample is removed from the supernatant by filtration or centrifugation, and then the concentration of the solute in the solution can be determined.

Different types of liquid phase composition analysis can be combined with the shake-flask method, such as High Performance Liquid Chromatography (HPLC), Ultraviolet–Visible spectrophotometry (UV-Vis) and gravimetry. The gravimetric method of analysis is usually quite accurate and reproducible. However, after preliminary tests with *trans*-cinnamic acid, some degradation phenomena were observed. After placing a *trans*-cinnamic acid sample in an oven at 70 °C, a weight loss of around 6.3% was measured after one week, with color change from white to yellow. Under the same oven conditions, for *p*-coumaric acid and ferulic acid, less significant weight losses of 0.01% and 0.14%, respectively, were obtained after one month, with no apparent color changes. Further gravimetric tests were performed at 30 °C, for *trans*-cinnamic acid, resulting in a weight loss of 0.25% after one week and 1.29% after one month, with no apparent color change. Therefore, UV-Vis spectroscopy was chosen as an alternative analytical technique, as the cinnamic acids absorb radiation between 200 nm and 400 nm. Nonetheless, to complement this data, the gravimetric method was also applied in some measurements, allowing a comparison between both methods of analysis.

To determine the optimal stirring time, preliminary experiments were also performed. A saturated solution of *trans*-cinnamic acid in water was placed in the thermostatic bath at 298.2 K and samples were taken at different times until the equilibrium concentration was achieved. The optimum stirring time is lower than 32 hours, as can be seen in Figure 3.1.

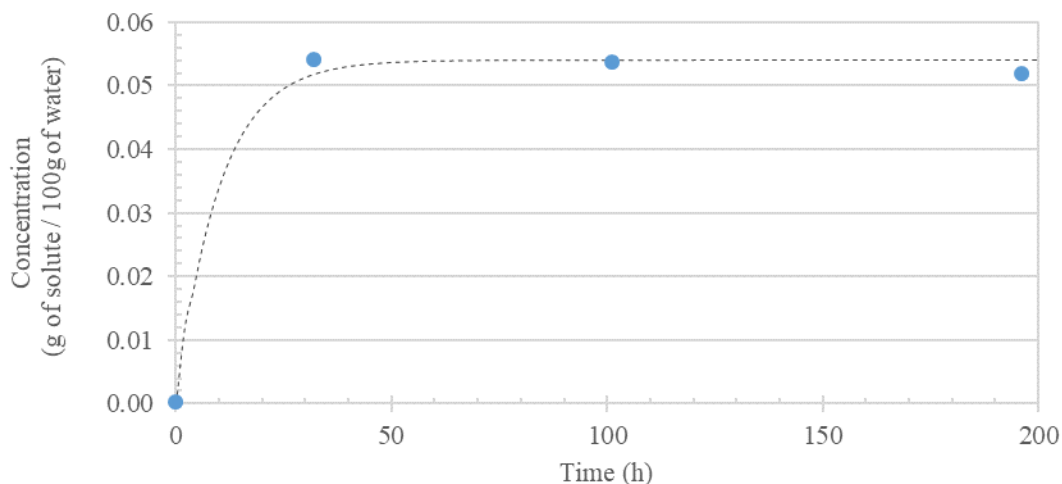


Figure 3.1 Solubility of *trans*-cinnamic acid in water as a function of stirring time. The line is a guide for the eyes.

The saturated solutions were prepared by mixing a small amount of solid in excess to the Erlenmeyer flasks containing between 20 mL and 30 mL of solvent. The flasks were covered with aluminum foil to protect solutions from possible light degradation and, then, placed under magnetic stirring inside a thermostatic bath (Lauda Instruments, model E20, Ecoline 025). The experiments were carried out at 298.2 K and 313.2 K, and it was possible to guarantee that the temperature of the solution was within ± 0.1 K, as described in detail elsewhere (Ferreira and Pinho, 2012).

For the systems with no data available in literature, for example, systems with 2-butanone and acetonitrile, preliminary experiments were performed at ambient temperature by placing the flasks directly over a plate stirrer (Magnetic Stirrer MSH-300N, BOECO Germany) during 2 hours to 3 hours. After reaching a saturated solution with a small quantity of solid in excess, the flasks were placed in the bath for the remaining stirring period.

After a settling period of at least 14.5 hours, three samples with a volume between 0.2 mL and 0.3 mL were collected from the supernatant solution, using pre-heated plastic syringes with metal needles and placed in a pre-weighed glass flask. The third sample was collected and filtered with pre-heated polypropylene filters (0.45 μm pore diameter). In selected cases, for comparison purposes, a fourth sample with a volume varying between 1.0 mL and 2.0 mL was also taken for gravimetric analysis. After the samples were taken from the solution and placed into small flasks, these were immediately covered with a screw cap and weighed.

The first three samples were diluted to a concentration of order of magnitude between 10^{-6} and 10^{-5} in a mixture of water + ethanol (35:65, wt.%) and read in the UV-Vis (T70 UV/VIS Spectrometer – PG Instruments Ltd) using the appropriate wavelength determined for each compound, and reported in Table 3.2. The UV-Vis calibration curves are available in Appendix D. The standard solutions of the calibration curves were prepared in a mixed ethanol-water solvent, due to the low water solubilities.

Table 3.2 Wavelengths used for UV-Vis spectrophotometry measurements.

Component	Wavelength (nm)
<i>trans</i> -cinnamic acid	273
<i>p</i> -coumaric acid	310
ferulic acid	321

The fourth sample, analyzed by gravimetry, was put in a hood until all the visible solvent evaporated. Afterwards, the sample was transferred to an oven operating at 303.2 K, for at least 7 days. Then, the samples were taken from the oven and placed into a desiccator for 1 hour, and then weighted in an analytical balance (TB 224A - Denver Instrument). This procedure was repeated once a week, for each sample, until a constant mass was reached. The average required time to obtain completely dried samples was 3 weeks.

3.3. Results and Discussion

3.3.1. Melting Properties

Table 3.3 presents the results of the measurements of the melting properties performed in this work in comparison to the literature average values. For *trans*-cinnamic acid, the measurements carried out in this work are in close agreement with literature. It was not possible to measure the melting properties of *p*-coumaric acid, because apparently a recrystallization occurred shortly after the melting. Furthermore, the decomposition of *p*-CA upon melting was also reported in literature (Dávalos *et al.*, 2012). The measured melting temperature of ferulic acid is in close agreement with literature, but the melting enthalpy measured here was higher than the literature average which suggests further studies.

For the *trans*-cinnamic acid, cyclic measurements were carried out, in which the melting properties were measured three times in sequence. In this measurement a possible degradation was observed because there was a reduction of the area of the peaks.

For the ferulic acid, the thermograms showed one endothermic peak and a linear baseline could be made to calculate the temperature melting and the peak area in the first measurement, but it was not possible to measure the melting properties in cyclic measurements, as the *trans*-cinnamic acid, because the recrystallization appeared to occur in a different crystal structure. The thermograms are shown in Appendix E.

Table 3.3 Comparison between the melting properties measured in this work and the average literature values.

Compound	T_m (K)	$\Delta_m H$ (kJ mol ⁻¹)	Reference
<i>trans</i> -cinnamic acid	405.80 ± 0.67	22.42 ± 0.24	Average value
	406.91 ± 0.17	21.90 ± 0.28	This work
<i>p</i> -coumaric acid	493.35 ± 1.41	30.86 ± 4.86	Average value
	NA ^a	NA ^a	This work
ferulic acid	445.64 ± 1.25	33.94 ± 1.64	Average value
	446.09 ± 0.53	41.10 ± 0.74	This work

^aNot available.

3.3.2. Solubility Measurements

Tables 3.4 to 3.7 present the solubility measured in this work for *trans*-cinnamic acid, *p*-coumaric acid and ferulic acid in water and organic solvents by UV-Vis spectroscopy (Tables 3.4 and 3.5) and gravimetry (Tables 3.6 and 3.7), at 298.2 K and 313.2 K.

Table 3.4 Solubility (g of solute per 100 g of solvent) of the studied cinnamic acids at 298.2 K in water and organic solvents measured by UV-Vis spectroscopy.

Solvent	<i>t</i> -CA	<i>p</i> -CA	FA
water	0.046 ± 0.001	0.054 ± 0.001	0.055 ± 0.001
methanol	33.115 ± 0.951	21.068 ± 0.466	15.328 ± 1.097
ethanol	27.248 ± 1.186	17.651 ± 1.214	10.389 ± 0.309
1-propanol	17.638 ± 0.765	10.041 ± 0.280	4.978 ± 0.267
2-propanol	18.033 ± 1.051	8.742 ± 0.284	5.374 ± 0.060

Table 3.4 (Continued).

Solvent	<i>t</i>-CA	<i>p</i>-CA	FA
2-butanone	23.728 ± 0.142	7.346 ± 0.403	7.317 ± 0.221
ethyl acetate	13.761 ± 0.241	1.915 ± 0.197	2.538 ± 0.074
acetonitrile	6.735 ± 0.030	1.043 ± 0.040	1.867 ± 0.066

Table 3.5 Solubility (g of solute per 100 g of solvent) of the studied cinnamic acids at 313.2 K in water and organic solvents measured by UV-Vis spectroscopy.

Solvent	<i>t</i>-CA	<i>p</i>-CA	FA
water	0.088 ± 0.001	0.127 ± 0.004	0.112 ± 0.003
methanol	48.586 ± 1.953	28.938 ± 0.667	27.512 ± 0.371
ethanol	40.469 ± 0.112	25.209 ± 0.984	17.538 ± 2.251
1-propanol	30.856 ± 0.147	10.378 ± 0.278	8.196 ± 0.308
2-propanol	32.466 ± 0.574	9.651 ± 0.293	8.135 ± 0.532
2-butanone	34.988 ± 1.111	9.068 ± 0.381	10.345 ± 0.419
ethyl acetate	21.601 ± 0.200	2.602 ± 0.045	3.998 ± 0.065
acetonitrile	12.059 ± 0.171	1.790 ± 0.032	2.879 ± 0.085

Table 3.6 Solubility (g of solute per 100 g of solvent) of the studied cinnamic acids in water and organic solvents at 298.2 K measured by gravimetry.

Solvent	<i>p</i>-CA	FA
water	0.0302	0.0238
methanol	22.8953	-
ethanol	18.2201	11.4590
1-propanol	10.8813	5.6819
2-propanol	9.5636	5.8741
2-butanone	9.1669	8.8635
ethyl acetate	2.4025	3.1912
acetonitrile	1.2630	2.1183

Table 3.7 Solubility (g of solute per 100 g of solvent) of the studied cinnamic acids in water and selected organic solvents at 313.2 K measured by gravimetry.

Solvent	<i>p</i> -CA	FA
2-propanol	10.1507	-
ethyl acetate	2.7463	4.5095
acetonitrile	2.0151	3.6821

The solubilities in water measured by gravimetry were lower than the solubilities measured by UV-Vis spectroscopy, probably due to the low solubility of these compounds in water, which makes it more difficult to measure the solubility by the gravimetric method.

Concerning the organic solvents, the gravimetric solubilities were slightly higher in comparison to the solubilities measured by UV-Vis spectroscopy, this behavior was also observed in the literature results, for example, in the case of the ferulic acid + ethanol system at 298.2 K, Bitencourt *et al.* (2016) used the gravimetric method and obtained solubility of 11.25 g of solute per 100 g of solvent, on the other hand Shakeel *et al.* (2017) measured by UV-Vis spectroscopy obtained 10.41 g of solute per 100 g of solvent, values that are in close agreement with the solubilities measured in this work by the different methods.

In general, as the temperature increases, the solubility also increases. This variation is stronger in aqueous systems than in organic solvents. The solubility of *p*-coumaric acid in 1-propanol and 2-propanol increased 3.25% and 9.42%, respectively, a low percentage when compared with the increase for the *trans*-cinnamic acid (42.84% and 44.46%) and ferulic acid (39.26% and 33.94%). Therefore, further studies should be performed to verify the results obtained for these systems.

The bubble graphics shown in Figure 3.2 were drawn to better compare the solubility of these phenolic compounds in the different solvents. The binary systems containing *trans*-cinnamic acid present the highest solubilities in the organic solvents. By calculating the ideal solubility using Equation 6, the following order is found $x_{p-CA} < x_{FA} < x_{l-CA}$. But, of course, the molecular interactions in solution will also have a major contribution in the solubility behavior.

p-Coumaric acid is more soluble in alcohols than ferulic acid, while in all other organics is the opposite. It probably occurs due to the molecular structure of *p*-CA, as the hydroxyl group is less hindered, allowing to establish stronger hydrogen bonds compared to ferulic acid, which also

has the methoxy group in the third position of the aromatic ring. The solubility of *p*-CA is higher in 1-propanol than in 2-propanol, because the two methyl groups of the latter again may hinder the OH group.

In the case of water, *trans*-cinnamic acids is the least soluble at both temperatures. Ferulic acid and *p*-coumaric acid have very close solubilities at 298.2 K, having *p*-CA a higher increase in the solubility with temperature. The highest solubility for all acids occurs in methanol.

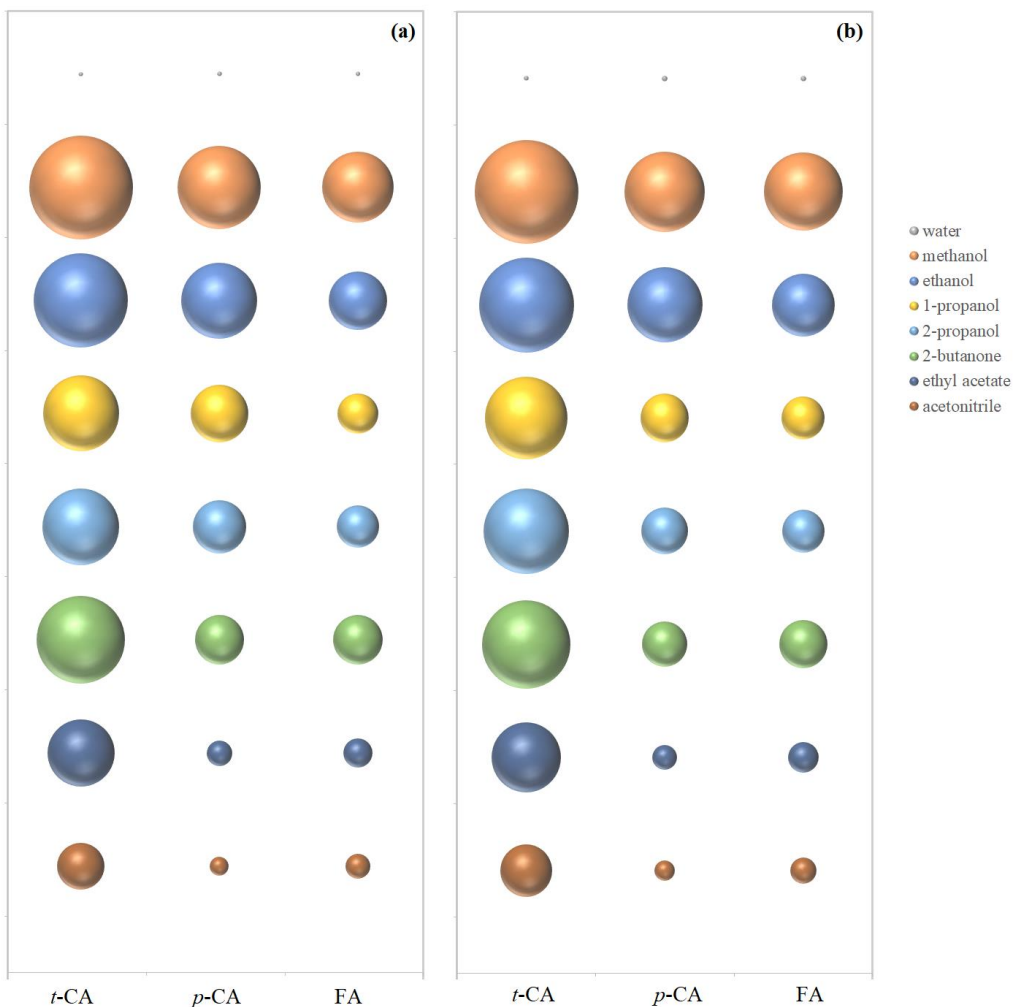


Figure 3.2 Solubility of the cinnamic acids in water and organic solvents measured by UV-Vis spectroscopy at (a) 298.2 K and (b) 313.2 K.

In order to better evaluate the experimental results obtained in this work, a comparison with the available literature data is shown in Figures 3.3 to 3.5. In general, when results by different authors are available, they are consistent with each other, with some exceptions.

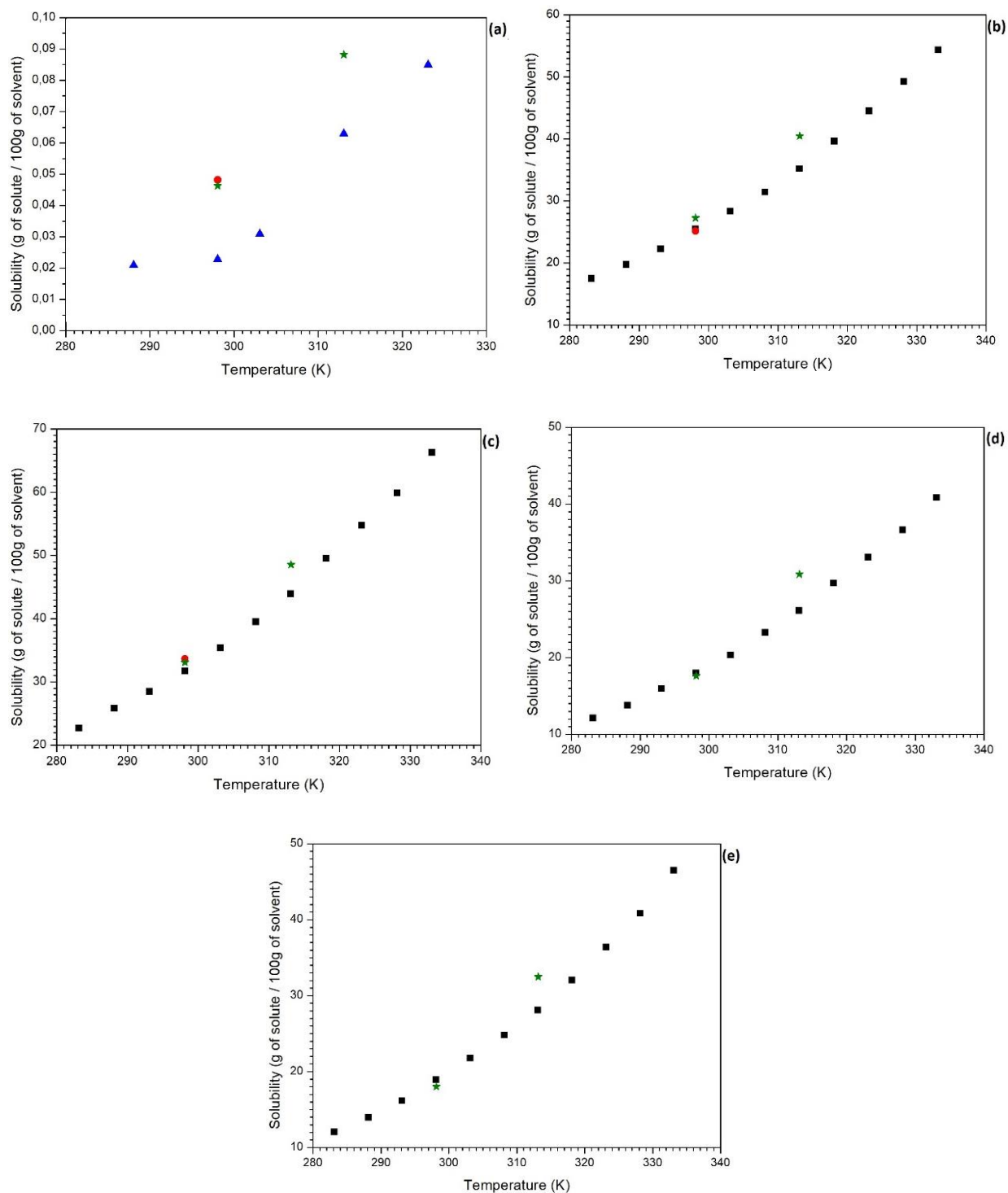


Figure 3.3 Solubility of *trans*-cinnamic acid in water and organic solvents (a) water, (b) ethanol, (c) methanol, (d) 1-propanol and (e) 2-propanol as function of temperature: (■) (Li *et al.*, 2016), (●) (Soares, 2017), (▲) (Mota *et al.*, 2008) and (★) this work.

The solubility of *trans*-cinnamic acid in water reported by Mota *et al.* (2008) at 298.2 K is lower than the result reported by Soares (2017), while this last is in very good agreement to the value found in this work. At 313.2 K the value here reported is again higher than that from Mota *et al.* (2008), which shows a rather unusual solubility change with temperature. The shake-flask methodology coupled to UV-Vis spectrophotometric analysis was applied in both studies. The main difference between the methodologies are the stirring and settling times. Mota *et al.* (2008) allowed samples to stir for up to 156 hours and the settling time was 42 hours, while Soares (2017) applied 30 hours of stirring time and 12 hours of settling time, where the methodology applied by Soares (2017) is similar to the one applied in this work; 32 hours for stirring and 15 hours for settling. Therefore, the higher solubility found here could only be explained by the shorter settling time, but the use of the polypropylene filters would avoid the sampling of any particle not dissolved.

The solubility of *t*-CA in ethanol, methanol, 1-propanol and 2-propanol at 298.2 K are consistent with literature data. On the other hand, at 313.2 K, the solubilities measured in this work are 12.8% higher, on average, than the values reported by Li *et al.* (2016). Li *et al.* (2016) measured the solubilities by a synthetic method, the last crystal disappearance method, with a stirring time of 2 hours, a much lower time than the one applied in this work.

The solubilities of *p*-coumaric acid are shown in Figure 3.8. The results obtained in the solvents ethanol and methanol at both temperatures, and 1-propanol and 2-propanol at 298.2 K are in close agreement with the literature. At 313.2 K the solubilities for 1-propanol and 2-propanol are lower than the literature, but as stated earlier, further studies should be performed to verify the results obtained for these systems.

For solubility of *p*-CA in ethyl acetate, the values obtained in this work are lower than literature values. Alevizou and Voutsas (2013) used the saturation method in a Thermomixer Comfort coupled to HPLC and UV-Vis with stirring time of 24 hours to 192 hours and non-reported settling time, and Ji *et al.* (2016) measured the solubilities using the shake-flask coupled to gravimetric method with 72 hours of stirring time and 12 hours of settling time. As previously reported, the results obtained from the gravimetry method generally are higher than the UV-Vis spectroscopy. In addition, according to a study carried out by Baka *et al.* (2008), in which all the variables of the shake-flask method were tested, for the measurement of solubility the settling time is more significant than the stirring time, which is longer in the methodology applied in this work.

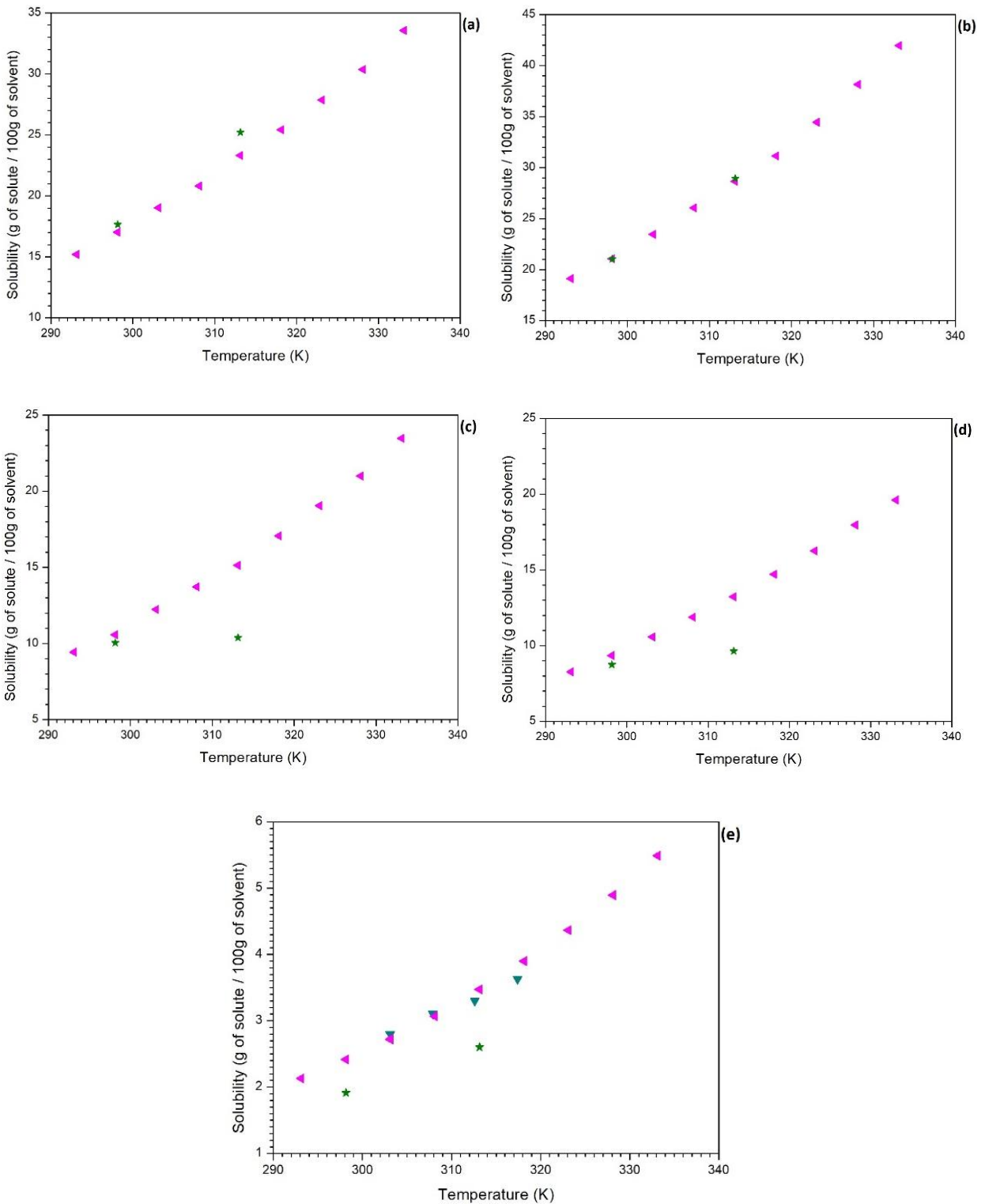


Figure 3.4 Solubility of *p*-coumaric acid in water and organic solvents (a) ethanol, (b) methanol, (c) 1-propanol, (d) 2-propanol and (e) ethyl acetate as function of temperature: (▲) (Ji *et al.*, 2016), (▼) (Alevizou and Voutsas, 2013) and (★) this work.

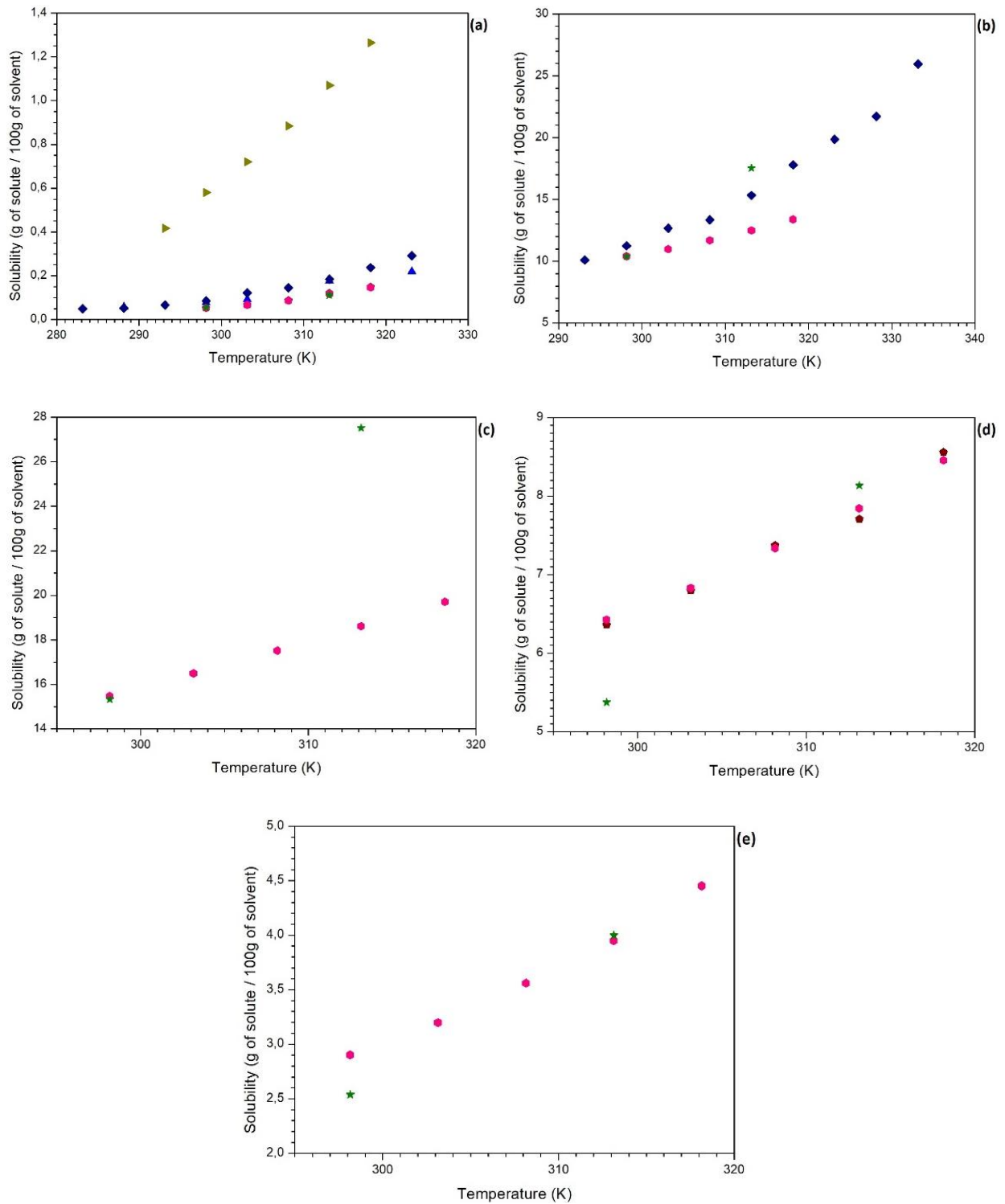


Figure 3.5 Solubility of ferulic acid in water and organic solvents (a) water, (b) ethanol, (c) methanol, (d) 2-propanol and (e) ethyl acetate as function of temperature: (◆) (Bitencourt *et al.*, 2016), (●) (Shakeel *et al.*, 2017), (▲) (Noubigh *et al.*, 2007), (◆) (Haq *et al.*, 2017), (▲) (Mota *et al.*, 2008) and (★) this work.

Ferulic acid has the largest amount of solubility data available in the literature, being also one of the most abundant phenolic acids in nature. Although solubility measurements of ferulic acid were performed by several authors, the values do not totally agree. For example, the solubility of ferulic acid in water provided by Noubigh *et al.* (2007) is generally much higher than the results reported by Mota *et al.* (2008), Bitencourt *et al.* (2016), Shakeel *et al.* (2017), Haq *et al.* (2017) and in this work. Shakeel *et al.* (2017) and Haq *et al.* (2017) also applied the shake-flask methodology coupled to RP-HPLC with UV-Vis spectroscopy, Mota *et al.* (2008) and Bitencourt *et al.* (2016) applied the shake-flask methodology coupled to gravimetric method. Finally, Noubigh *et al.* (2007) also applied the shake-flask methodology, but coupled with HPLC, with stirring and settling times of 3 hours, shorter times compared to other methodologies which should have given lower solubilities. Therefore, other factors should be looked for to explain the differences.

The remaining solubility data of FA in ethanol, 2-propanol and ethyl acetate at both temperatures, and methanol at 298.2 K are in agreement with literature. However, the solubility of ferulic acid in methanol at 313.2 K, compared to the solubility measured by Shakeel *et al.* (2017), was 32.3% higher requiring further measurements at this temperature. Complementary, X-ray studies of the crystal phases in equilibrium should be carried out.

Chapter 4. Thermodynamic Modeling

4.1. The NRTL-SAC Model

The NRTL-SAC model and the estimation of the parameters for the three hydroxycinnamic acids were implemented using the software MATLAB version R2013a.

The main goal of the first set of simulations was to determine the four NRTL-SAC conceptual molecular segments (X , $Y+$, $Y-$, Z) for each solute, using some of the solubility data measured. After, those parameters were used to predict the solubility in a different set of solvents.

In order to evaluate the accuracy of the results obtained, the average relative deviations (ARD) were calculated for each binary system as follows:

$$ARD(\%) = \frac{1}{NP} \sum_i \frac{|x_i^{exp} - x_i^{calc}|}{x_i^{exp}} * 100 \quad (12)$$

where NP is the number of data points, and x_i^{exp} and x_i^{calc} are the experimental and calculated solubility in mole fraction, respectively.

For the optimization procedure, involving the application of Equation 6, the values of the melting properties presented in Table 3.3 were used but, for the *p*-coumaric and ferulic acids, the average values of literature were used, due to the difficulties for measuring the melting properties for the first acid, and the great discrepancy of the value measured for the enthalpy of melting ($\Delta_m H$) in this work, when compared to the literature.

For this correlation step, seven solvents (water, methanol, ethanol, 2-propanol, 2-butanone, ethyl acetate and acetonitrile) were selected. After, the parameters found were used to predict the solubility in 1-propanol, 1-butanol, isobutanol, 2-butanol, dimethyl sulfoxide (DMSO), acetone, methyl acetate and ethylene glycol. The experimental values for these solvents are from literature, except for 1-propanol (this work), and they are available in appendix (Table A.10).

Table 4.1 shows the optimized segment parameters and the global ARD for each solute studied in this work.

Table 4.1 NRTL-SAC optimized parameters and ARD (%) for each cinnamic acid using water and six organic solvents in the fitting.

Solute	X	Y+	Y-	Z	ARD (%)	ARD (%)
					Correlation	Prediction
<i>trans</i> -cinnamic acid	0.705	0.032	0.000	0.549	23	44
<i>p</i> -coumaric acid	0.574	0.809	0.937	1.292	39	42
ferulic acid	0.625	0.334	0.000	1.422	31	61

The prediction results show that the NRTL-SAC model is an adequate tool to estimate the solubility of the studied compounds, with minimum ARD value of 23% for *trans*-cinnamic acid and maximum ARD value of 39% for *p*-coumaric acid. In previous works, Mota *et al.* (2012) have applied this model to predict the solubility of drug molecules in different solvents, reporting ARD values between 18.4% and 59.6%, which are of the same order of magnitude of those found in this work.

Table 4.2 shows a summary of the ARD and the number of experimental data for each solvent used in the correlation and prediction steps and Figure 4.1 shows the comparison between experimental and calculated solubility.

Table 4.2 ARD (%) and experimental data (*NP*) for each solvent used in simulation.

Correlation			Prediction		
Solvent	ARD (%)	<i>NP</i>	Solvent	ARD (%)	<i>NP</i>
Water	10	6	1-butanol	30	6
methanol	21	6	2-butanol	56	2
ethanol	16	6	isobutanol	26	3
isopropanol	20	6	acetone	67	2
2-butanone	61	6	DMSO	155	2
ethyl acetate	60	6	ethylene glycol	60	2
acetonitrile	29	6	methyl acetate	89	2
			1-propanol	23	6

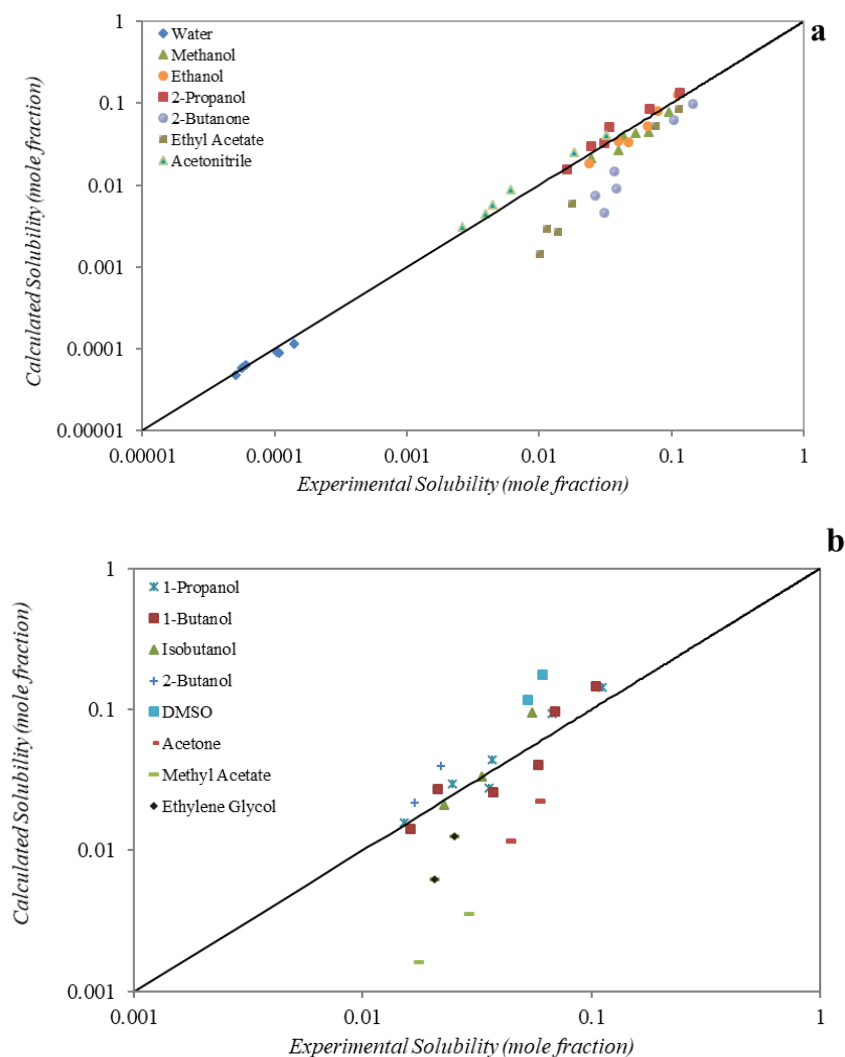


Figure 4.1 Comparison between experimental and calculated solubility using the NRTL-SAC model: (a) correlation; (b) prediction.

Better correlation results (ARD lower than 30%) were obtained in systems containing alcohols, water and acetonitrile, being 2-butanone and ethyl acetate the outliers with ARD close to 60%.

Regarding the predictions, the ARD for the solubility in alcohols are less than 30%, except for the prediction of 2-butanol, which presented 56%. Ketones and esters showed ARD between 60% and 87%, in line with the correlation values obtained for the same family of compounds. Finally, the prediction for DMSO stands out (ARD of 155%) which is not surprising considering the diverse chemical structure of the solvents included in the correlation database.

The Reference Solvent Approach (RSA) proposed by Abildskov and O’Connell (2003) was also coupled to the NRTL-SAC method as a second alternative to describe the solid-liquid equilibria, as the available temperature and enthalpy of melting are, in some cases, uncertain. The same optimization strategy was used, and Table 4.3 shows the estimated segment parameters and the general ARD for each solute studied in this work.

Table 4.3 NRTL-SAC + RSA approach optimized parameters and ARD (%) for each cinnamic acid using water and six organic solvents in the fitting.

Solute	X	Y+	Y-	Z	ARD (%) Correlation	ARD (%) Prediction
<i>trans</i> -cinnamic acid	0.701	0.084	0.000	0.598	27	32
<i>p</i> -coumaric acid	0.703	0.000	0.034	1.760	39	49
ferulic acid	0.642	0.302	0.000	1.456	34	73

Comparing the ARDs obtained earlier with those obtained using the reference solvent approach, the values are close, with ARD average values of 49% and 51% for predictions without and with the RSA coupled, respectively. In previous works, Mota *et al.* (2012) and Vilas-Boas *et al.* (2018) have applied the NRTL-SAC model with RSA to predict solubility of drug molecules and isomeric phenolic acids in different solvents, reporting ARD values of 14.1% to 58.9% and 28% to 40%, respectively, which are again of the same order of magnitude of those found in this work. For *trans*-cinnamic acid the outlier solvent was 2-butanone, in the case of ferulic acid it was acetonitrile, and for *p*-coumaric acid it was ethyl acetate. Regarding the set of parameters obtained with and without RSA, only for *p*-coumaric acid there was a significant difference between both sets which suggests the use of a larger database of solvents.

Figure 4.2 shows the comparison between experimental and calculated solubility and Table 4.4 shows de ARD and the number of experimental data for each solvent used in the correlation and prediction steps.

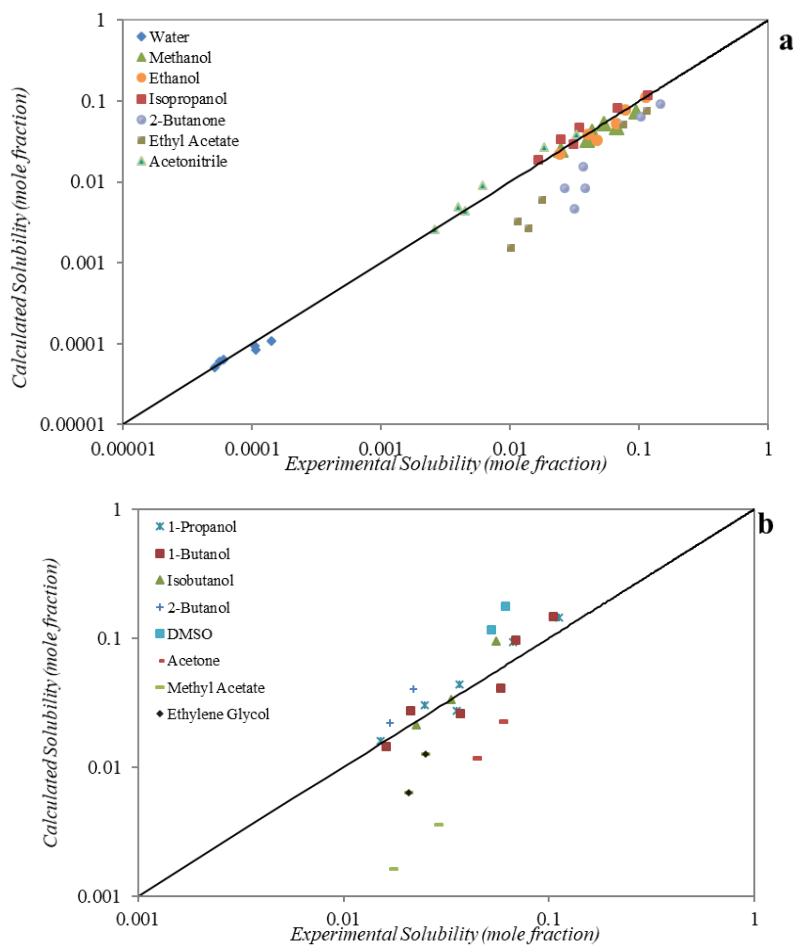


Figure 4.2 Comparison between experimental and calculated solubility using the NRTL-SAC model combined with the RSA: (a) correlation; (b) prediction.

Table 4.4 ARD (%) and number of experimental data (*NP*) for each solvent used in simulation.

Correlation			Prediction		
Solvent	ARD (%)	<i>NP</i>	Solvent	ARD (%)	<i>NP</i>
Water	11	6	1-butanol	36	6
methanol	11	6	2-butanol	26	2
ethanol	10	6	isobutanol	33	3
isopropanol	20	6	acetone	78	2
2-butanone	61	6	DMSO	176	2
ethyl acetate	62	6	ethylene glycol	79	2
acetonitrile	23	6	methyl acetate	97	2
			1-propanol	25	6

As before, the model predicts better for the alcohols, however, compared to the results for the NRTL-SAC without RSA, the ARD for all predictions were higher. Therefore, for this work, the application of the RSA methodology does not provide additional improvements.

4.2. The Abraham Solvation Model

Initially, the same set of organic solvents (methanol, ethanol, 2-propanol, 2-butanone and ethyl acetate) was used to estimate the parameters (S , A and B) from the Abraham solvation model. It should be mentioned that parameters E and V are calculated *a priori* using the equations available in Abraham *et al.* (2004). The physical properties used in those calculations are shown in Table 4.5. The complete set of parameters are presented in Table 4.6.

Table 4.5 Density at 25°C and refractive index of the cinnamic acids studied in this work.

Compound	Density (g/cm^3)	Refractive index at 20 °C ^a
<i>trans</i> -cinnamic acid	1.286 (Ladell <i>et al.</i> , 1956)	1.616
<i>p</i> -coumaric acid	1.403 (Kumar <i>et al.</i> , 2015)	1.660
ferulic acid	1.370 (Kumar and Pruthi, 2015)	1.626

^a Values calculated by the ACD software (ACD/ChemSketch, Advanced Chemistry Development Inc., 2017.1.2 version).

Table 4.6 Abraham estimated solute's parameters and ARD (%) for each hydroxycinnamic acid using water and six organic solvents in the fitting.

Solute	E	S	A	B	V	ARD (%) Correlation	ARD (%) Prediction
<i>trans</i> -cinnamic acid	1.301	1.212	0.622	0.468	1.171	7	4
<i>p</i> -coumaric acid	1.582	1.725	1.111	0.560	1.229	24	29
ferulic acid	1.537	1.609	0.644	0.802	1.429	15	940

Acree *et al.* (2017) applied the model in the experimental solubility measurements for *p*-coumaric acid published by Ji *et al.* (2016). The parameters calculated by them were $V = 1.2292$, $E = 1.330$, $S = 1.453$, $A = 0.841$ and $B = 0.674$. The E value is a function of the refractive index which has a great influence in this parameter. In this work, as mentioned before, we have used the ACD/ChemSketch software. As expected our values for S , A and B are slightly different from those published by Acree and co-workers, not only because of the different E value, but also by the higher number of solvents used in that work (9 pure solvents and 10 different proportions of the

water-ethanol mixed solvent). In addition, in this work, acetonitrile was also used in the correlation database.

As can be seen, for ferulic acid an atypical high ARD is obtained for the predictions. The outlier is the DMSO solvent, for which an ARD of 4662% is calculated. For this reason, a second optimization round was carried out only for this phenolic acid, by adding DMSO to the correlating set of solvents. The results obtained are presented in Table 4.7. The predictions improved significantly while maintaining the same ARD in the correlation results, showing again the importance of having a diverse chemical set of solvents to obtain more robust parameters.

Table 4.7 Abraham optimized solute's parameters and ARD (%) for ferulic acid using water and seven organic (including DMSO) solvents in the fitting.

Solute	<i>E</i>	<i>S</i>	<i>A</i>	<i>B</i>	<i>V</i>	ARD (%) Correlation	ARD (%) Prediction
ferulic acid	1.537	1.177	0.299	0.883	1.429	15	33

Finally, in Table 4.8, the global ARD are presented for each solvent and Figure 4.3 shows the comparison between experimental and calculated solubility.

Table 4.8 ARD (%) and number of points (*NP*) for each solvent used in simulation (second optimization round for ferulic acid).

Correlation			Prediction		
Solvent	ARD (%)	<i>NP</i>	Solvent	ARD (%)	<i>NP</i>
methanol	22	3	1-butanol	22	3
ethanol	9	3	2-butanol	15	1
isopropanol	5	3	isobutanol	16	2
2-butanone	9	3	acetone	26	1
ethyl acetate	37	3	ethylene glycol	49	1
acetonitrile	14	3	methyl acetate	34	1
DMSO	4	1	1-propanol	22	3

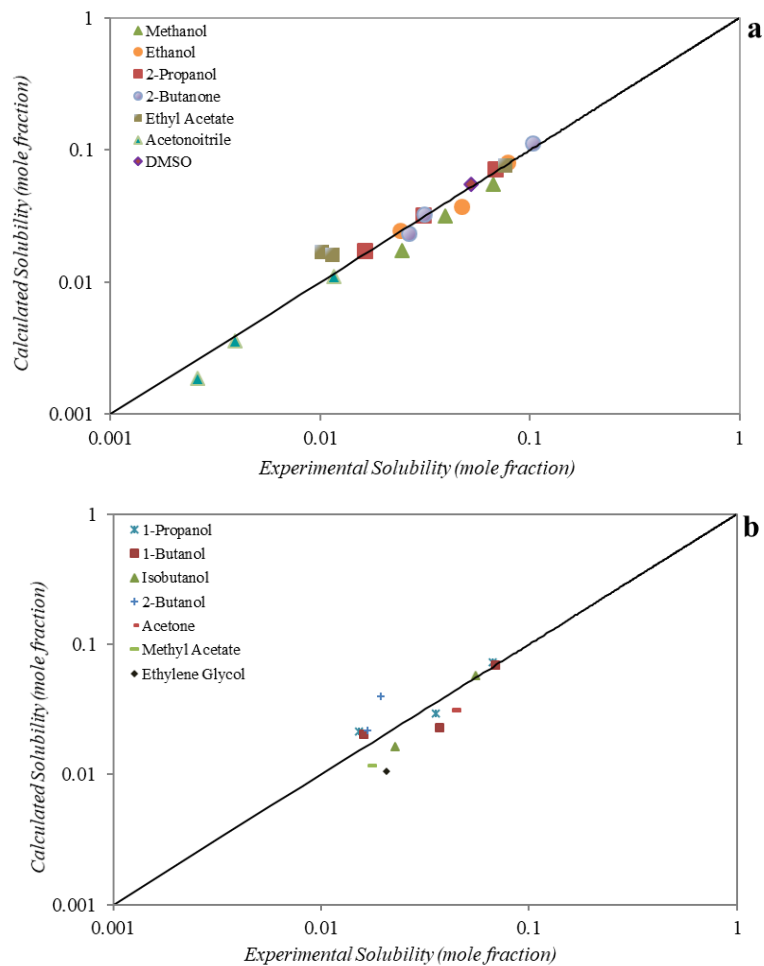


Figure 4.3 Comparison between experimental and calculated solubility using the Abraham solvation model: (a) correlation results; (b) predictions.

As can be seen, in general, the model shows a good ability to calculate the solubilities of the studied compounds, with the highest ARD of 37% for ethyl acetate in the correlation results and 34% and 49% for methyl acetate and ethylene glycol, respectively, for the predictions.

Chapter 5. Conclusions and Future Work

In this work, the solubility of *trans*-cinnamic acid, *p*-coumaric acid and ferulic acid was experimentally measured in water and different organic solvents (methanol, ethanol, 1-propanol, isopropanol, 2-butanone and ethyl acetate, acetonitrile), at 298.2 K and 313.2 K. The shake-flask methodology was applied using UV-Vis spectroscopy and the gravimetric methods of analysis. As the temperature increased, an increase in solubility was observed as the most common behaviour.

The solubility data generally exhibited the same pattern for alcohols, presenting the highest solubilities for those having the lowest carbon chain. An exception occurred for the system composed of *p*-coumaric acid and 1-propanol, at 298.2 K, for which the solubility value was higher than that obtained for the binary system containing 2-propanol, whereas for the *trans*-cinnamic and ferulic acids the solubility in the system containing 2-propanol was higher than in 1-propanol. Further experiments should be performed in the future to corroborate the values obtained in this work.

The melting points and enthalpies were also determined by DSC for the phenolic compounds discussed in this work. The results for the melting temperature were consistent with the literature values. In relation to the enthalpy of melting, the measured value for ferulic acid was considerably higher than the value published in the open literature.

The second important component of this work is the thermodynamic modeling, either applying the non-random liquid activity coefficient model (NRTL-SAC) or the Abraham's solvation model. The first model presented acceptable correlation results with average relative deviation (ARD) varying between 23% and 39%. After, the model was used to predict solubility in eight solvents and the ARD ranged from 42% to 61%. Contrarily the NRTL-SAC model coupled to RSA did not introduced significant improvement. The Abraham's solvation model presented ARD for the correlation between 7% and 24%, and for predictions between 4% and 33%, only after including the solubility in DMSO in the correlation database. This reinforces the importance of having a set of solvents with different functional groups to calculate the fitting parameters. In

general, for the solvents used in the simulations, the solubility in alcohols was better represented by the models, presenting the lowest ARD values.

The descriptors of the NRTL-SAC segment and the Abraham optimized solute's parameters calculated can contribute for future predictions in a much large variety of solvents. For further work, other experimental measures of solubility in different binary and multicomponent systems are suggested in order to provide greater robustness to the optimized parameters.

From the experimental point of view, besides some additional tests to confirm some solubility values measured in this work, the study of the solid phase, before and after dissolving the solute in several solvents, is envisaged. The eventual identification of different structures can also give some hints about the differences in the melting enthalpies. Also of high importance is to extend measurements to systems containing eutectic solvents and/or ionic liquids. The benchmark is to be able to use the data as well as the modelling results to screen a series of potential solvents that can compete with the usual water/alcohol solvent mixtures largely used to extract these compounds from natural matrices.

References

Abildskov, J. and O'Connell, J. P. (2005) 'Thermodynamic method for obtaining the solubilities of complex medium-sized chemicals in pure and mixed solvents', *Fluid Phase Equilibria*, 228–229, pp. 395–400.

Abraham, M. H., Acree Jr, W. E., Earp, C. E., Vladimirova, A. and Whaley, W. L. (2015) 'Studies on the hydrogen bond acidity, and other descriptors and properties for hydroxyflavones and hydroxyisoflavones', *Journal of Molecular Liquids*, 208, pp. 363–372.

Abraham, M. H., Ibrahim, A. and Zissimos, A. M. (2004) 'Determination of sets of solute descriptors from chromatographic measurements', *Journal of Chromatography A*, 1037, pp. 29–47.

Acree, W. E., Barrera, M. and Abraham, M. H. (2017) 'Comment on “measurement and correlation of the solubility of p-coumaric acid in nine pure and water + ethanol mixed solvents at temperatures from 293.15 to 333.15 K”', *Journal of Chemical and Engineering Data*, 62, pp. 578–583.

Acree, W. E. (1991) 'Thermodynamic properties of organic compounds: enthalpy of fusion and melting point temperature compilation', *Thermochimica Acta*, 189, pp. 37–56.

Alevizou, E. I. and Voutsas, E. C. (2013) 'Solubilities of p-coumaric and caffeic acid in ionic liquids and organic solvents', *The Journal of Chemical Thermodynamics*, 62, pp. 69–78.

Baka, E., Comer, J. E. A. and Takács-Novák, K. (2008) 'Study of equilibrium solubility measurement by saturation shake-flask method using hydrochlorothiazide as model compound', *Journal of Pharmaceutical and Biomedical Analysis*, 46, pp. 335–341.

Bevill, M. J., Vlahoa, P. I. and Smit, J. P. (2014) 'Polymorphic cocrystals of nutraceutical compound p-coumaric acid with nicotinamide: Characterization, relative solid-state stability, and conversion to alternate stoichiometries', *Crystal Growth & Design*, 14, pp. 1438–1448.

Bitencourt, R. G., Cabral, F. A. and Meirelles, A. J. A. (2016) 'Ferulic acid solubility in supercritical carbon dioxide, ethanol and water mixtures', *The Journal of Chemical Thermodynamics*, 103, pp. 285–291.

Bravo, L. (1998) 'Polyphenols: chemistry, dietary sources, metabolism, and nutritional significance', *Nutrition Reviews*, 56, pp. 317–333.

Chen, C. C., and Song, Y. (2004) ‘Solubility modeling with a nonrandom two-liquid segment activity coefficient model’, *Industrial & Engineering Chemistry Research*, 43, pp. 8354–8362.

Chen, C. C., Simoni, L. D., Brennecke, J. F., and Stadtherr, M. A. (2008) ‘Correlation and prediction of phase behavior of organic compounds in ionic liquids using the nonrandom two-liquid segment activity coefficient model’, *Industrial & Engineering Chemistry Research*, 47, pp. 7081–7093.

Cheng, Z. Y., Sun, L., Wang, X. J., Sun, R., An, Y. Q., An, B. L., Zhu, M. X., Zhao, C. F., and Bai, J. G. (2018) ‘Ferulic acid pretreatment alleviates heat stress in blueberry seedlings by inducing antioxidant enzymes, proline, and soluble sugars’, *Biologia Plantarum*, 62, pp. 534–542.

Dávalos, J. Z., Herrero, R., Chana, A., Guerrero, A., Jiménez, P., and Santiuste, J. M. (2012) ‘Energetics and structural properties, in the gas phase, of trans-hydroxycinnamic acids’, *The Journal of Physical Chemistry A*, 116, pp. 2261–2267.

Emel’yanenko, V. N., Yermalayeu, A. V., Voges, M., Held, C., Sadowski, G., and Verevkin, S. P. (2016) ‘Thermodynamics of a model biological reaction: A comprehensive combined experimental and theoretical study’, *Fluid Phase Equilibria*, 422, pp. 99–110.

Ezhuthupurakkal, P. B., Ariraman, S., Arumugam, S., Subramaniyan, N., Muthuvel, S. K., Kumpati, P., Rajamani, B., and Chinnasamy, T. (2018) ‘Anticancer potential of ZnO nanoparticle-ferulic acid conjugate on Huh-7 and HepG2 cells and diethyl nitrosamine induced hepatocellular cancer on Wistar albino rat’, *Nanomedicine: Nanotechnology, Biology, and Medicine*, 14, pp. 415–428.

Ferreira, P. S., Victorelli, F. D., Fonseca-Santos, B., and Chorilli, M. (2018) ‘A review of analytical methods for p-coumaric acid in plant-based products, beverages, and biological matrices’, *Critical Reviews in Analytical Chemistry*, doi: 10408347.2018.1459173.

Ferreira, O. and Pinho, S. P. (2012) ‘Solubility of flavonoids in pure solvents’, *Industrial and Engineering Chemistry Research*, 51, p. 6586–6590.

Ferreira, O., Schröder, B. and Pinho, S. P. (2013) ‘Solubility of hesperetin in mixed solvents’, *Journal of Chemical and Engineering Data*, 58, pp. 2616–2621.

Haq, N., Siddiqui, N. A. and Shakeel, F. (2017) ‘Solubility and molecular interactions of ferulic acid in various (isopropanol + water) mixtures’, *Journal of Pharmacy and Pharmacology*, 69, pp. 1485–1494.

Hefter, G. T. and Tomkins, R. P. T. (2003) *The experimental determination of solubilities*. John Wiley & Sons, LTD.

Ji, W., Meng, Q., Ding, L., Wang, F., Dong, J., Zhou, G., and Wang, B. (2016) 'Measurement and correlation of the solubility of caffeic acid in eight mono and water + ethanol mixed solvents at temperatures from (293.15 to 333.15) K', *Journal of Molecular Liquids*, 224, pp. 1275–1281.

Ji, W., Meng, Q., Li, P., Yang, B., Ding, L., Wang, B., and Wang, F. (2016) 'Measurement and correlation of the solubility of p-coumaric acid in nine pure and water + ethanol mixed solvents at temperatures from 293.15 to 333.15 K', *Journal of Chemical and Engineering Data*, 61, pp. 3457–3465.

Jia, S. R., Cui, J. D., Li, Y., and Sun, A. Y. (2008) 'Production of l-phenylalanine from trans-cinnamic acids by high-level expression of phenylalanine ammonia lyase gene from *Rhodospiridium toruloides* in *Escherichia coli*', *Biochemical Engineering Journal*, 42, pp. 193–197.

Kim, A., Im, M., Gu, M. J., and Ma, J. Y. (2016) 'Ethanol extract of *Lophatheri Herba* exhibits anti-cancer activity in human cancer cells by suppression of metastatic and angiogenic potential', *Scientific Reports*, 6, 36277.

Kumar, N. and Pruthi, V. (2015) 'Structural elucidation and molecular docking of ferulic acid from *Parthenium hysterophorus* possessing COX-2 inhibition activity', *3 Biotech*, 5, pp. 541–551.

Kumar, N., Pruthi, V. and Goel, N. (2015) 'Structural, thermal and quantum chemical studies of p-coumaric and caffeic acids', *Journal of Molecular Structure*, 1085, pp. 242–248.

Ladell, J., McDonald, T. R. R. and Schmidt, G. M. J. (1956) 'The crystal structure of α -trans -cinnamic acid', *Acta Crystallographica*, p. 195.

Li, J., Zeng, Z. X., Sun, L., Xue, W. L., and Wang, H. H. (2016) 'Solid-liquid phase equilibrium of trans-cinnamic acid in several alcohols: measurements and thermodynamic modeling', *Journal of Chemical and Engineering Data*, 61, pp. 1192–1198.

Manic, M. S., Villanueva, D., Fornari, T., Queimada, A. J., Macedo, E. A., and Najdanovic-Visak, V. (2012) 'Solubility of high-value compounds in ethyl lactate: Measurements and modeling', *Journal of Chemical Thermodynamics*, 48, pp. 93–100.

Martins, C. R., Lopes, W. A. and De Andrade, J. B. (2013) 'Solubilidade das substâncias

orgânicas’, *Quimica Nova*, 36, pp. 1248–1255.

Mathew, S. and Abraham, T. E. (2004) ‘Ferulic acid: An antioxidant found naturally in plant cell walls and feruloyl esterases involved in its release and their applications’, *Critical Reviews in Biotechnology*, 24, pp. 59–83.

Mota, F. L., Queimada, A. J., Andreatta, A. E., Pinho, S. P. and Macedo, E. A. (2012) ‘Calculation of drug-like molecules solubility using predictive activity coefficient models’, *Fluid Phase Equilibria*, 322–323, pp. 48–55.

Mota, F. L., Queimada, A. J., Pinho, S. P., and Macedo, E. A. (2008) ‘Aqueous solubility of some natural phenolic compounds’, *Industrial and Engineering Chemistry Research*, 47, pp. 5182–5189.

Noubigh, A., Abderrabba, M. and Provost, E. (2007) ‘Temperature and salt addition effects on the solubility behaviour of some phenolic compounds in water’, *Journal of Chemical Thermodynamics*, 39, pp. 297–303.

Ou, S. and Kwok, K. C. (2004) ‘Ferulic acid: Pharmaceutical functions, preparation and applications in foods’, *Journal of the Science of Food and Agriculture*, 84, pp. 1261–1269.

Pacheco-Palencia, L. A., Mertens-Talcott, S. and Talcott, S. T. (2008) ‘Chemical composition, antioxidant properties, and thermal stability of a phytochemical enriched oil from açai (*Euterpe oleracea* Mart.)’, *Journal of Agricultural and Food Chemistry*, 56, pp. 4631–4636.

Papadopoulos, G. and Boskou, D. (1991) ‘Antioxidant effect of natural phenols on olive oil’, *Journal of the American Oil Chemists Society*, 68, pp. 669–671.

Peng, J., Zheng, T-T., Liang, Y., Duan, L-F., Zhang, Y-D., Wang, L-J., He, G-M., and Xiao, H.-T. (2018) ‘p-Coumaric acid protects human lens epithelial cells against oxidative stress-induced apoptosis by MAPK signaling’, *Oxidative Medicine and Cellular Longevity*, 2018, Article ID 8549052, 7 pages.

Renon, H. and Prausnitz, J. M. (1968) ‘Local Compositions in Thermodynamic Excess Functions for Liquid Mixtures.’, *AIChE Journal*, 14, pp. 135–144.

Shakeel, F., Salem-Bekhit, M. M., Haq, N., and Siddiqui, N. A. (2017) ‘Solubility and thermodynamics of ferulic acid in different neat solvents: Measurement, correlation and molecular interactions’, *Journal of Molecular Liquids*, 236, pp. 144–150.

Soares, B. D. P. (2017) ‘Medições de Solubilidade de Compostos Pouco Solúveis em Água’, *Dissertation of Master Degree in Chemical Engineering at Instituto Politécnico de*

Bragança, Portugal.

Stalikas, C. D. (2007) 'Extraction, separation, and detection methods for phenolic acids and flavonoids', *Journal of Separation Science*, 30, pp. 3268 – 3295.

Vilas-Boas, S.M., Brandão, P., Martins, M.A.R., Silva, L.P., Schreiner, T.B., Fernandes, L., Ferreira, O. and Pinho, S. P. (2018) 'Solubility and solid phase studies of isomeric phenolic acids in pure solvents', *Journal of Molecular Liquids*, 272, pp. 1048–1057.

Vilas-Boas, S. M. (2017) 'Studies on the Solubility of phenolic compounds', *Dissertation of Master Degree in Chemical Engineering at Instituto Politécnico de Bragança*, Portugal.

Wang, H., Li, Q., Deng, W., Omari-Siaw, E., Wang, Q. and Wang, S., Wang, S., Cao, X., Xu, X., and Yu, J. (2015) 'Self-nanoemulsifying drug delivery system of trans-cinnamic acid: Formulation development and pharmacodynamic evaluation in alloxan-induced type 2 diabetic rat model', *Drug Development Research*, 76, pp. 82–93.

Yen, G. C., Chen, L.Y., Sun, F. M., Chiang, Y. L., Lu, S. H., and Weng, C. J. (2011) 'A comparative study on the effectiveness of cis- and trans-form of cinnamic acid treatments for inhibiting invasive activity of human lung adenocarcinoma cells', *European Journal of Pharmaceutical Sciences*, 44, pp. 281–287.

Appendix A: Literature Solubility Data of *t*-CA, *p*-CA and FA

The following tables present the solubility data found in literature of *trans*-cinnamic acid, *p*-coumaric acid and ferulic acid in water and organic solvents.

Table A.1 Solubility in mole fraction of *trans*-cinnamic acid in organic solvents measured by Li *et al.* (2016).

Temperature (K)	Solubility $\times 10^2$ (mole fraction)			
	Methanol	Ethanol	1-Propanol	2-Propanol
283.15	4.68	5.15	4.69	4.65
288.15	5.30	5.78	5.30	5.35
293.15	5.81	6.48	6.08	6.15
298.15	6.42	7.33	6.80	7.12
303.15	7.10	8.09	7.61	8.11
308.15	7.87	8.90	8.62	9.14
313.15	8.68	9.86	9.57	10.23
318.15	9.67	10.96	10.75	11.50
323.15	10.58	12.15	11.83	12.86
328.15	11.47	13.27	12.93	14.21
333.15	12.53	14.45	14.21	15.86

Table A.2 Solubility in g/L of *trans*-cinnamic acid in water.

Temperature (K)	Solubility (g/L)	Reference
288.15	0.21 \pm 0.01	(Mota <i>et al.</i> , 2008)
298.15	0.23 \pm 0.01	
303.15	0.31 \pm 0.01	
313.15	0.63 \pm 0.02	
323.15	0.85 \pm 0.02	
298.15	0.483 \pm 0.006	(Soares, 2017)

Table A.3 Solubility (g of solute per 100 g of solvent) of *trans*-cinnamic acid in methanol and ethanol, measured by Soares (2017).

Temperature (K)	Solubility (g of solute / 100 g of solvent)	
	Methanol	Ethanol
298.15	25.16	33.64

Table A.4 Solubility in mole fraction of *p*-coumaric acid in ethyl acetate.

Temperature (K)	Solubility (mole fraction)	Reference
303.10	0.0148	
307.90	0.0164	(Alevizou and Voutsas, 2013)
312.60	0.0174	
317.40	0.0191	
293.15	0.0113	
298.15	0.0128	
303.15	0.0144	
308.15	0.0162	
313.15	0.0183	(Ji <i>et al.</i> , 2016)
318.15	0.0205	
323.15	0.0229	
328.15	0.0256	
333.15	0.0286	

Table A.5 Solubility in mole fraction of *p*-coumaric acid in organic solvents measured by Ji *et al.* (2016).

Temperature (K)	Solubility $\times 10^2$ (mole fraction)			
	Methano	Ethanol	1-Propanol	2-Propanol
293.15	3.60	4.09	3.34	2.94
298.15	3.95	4.56	3.73	3.31
303.15	4.38	5.07	4.29	3.73
308.15	4.84	5.52	4.78	4.17
313.15	5.30	6.14	5.25	4.62
318.15	5.73	6.66	5.88	5.11
323.15	6.30	7.25	6.52	5.62
328.15	6.93	7.85	7.14	6.17
333.15	7.57	8.61	7.91	6.70

Table A.6 Solubility in mole fraction of ferulic acid in organic solvents.

Solvent	Temperature (K)	Solubility $\times 10^2$ (mole fraction)	Reference
methanol	298.2	2.49	(Shakeel <i>et al.</i> , 2017)
	303.2	2.65	
	308.2	2.81	
	313.2	2.98	
	318.2	3.15	
	298.2	2.41	(Shakeel <i>et al.</i> , 2017)
	303.2	2.54	
	308.2	2.70	
	313.2	2.88	
	318.2	3.08	
ethanol	293	2.34 ± 0.02	(Bitencourt <i>et al.</i> , 2016)
	298	2.60 ± 0.01	
	303	2.92 ± 0.01	
	308	3.07 ± 0.03	
	313	3.51 ± 0.06	
	318	4.05 ± 0.03	
	323	4.5 ± 0.1	
	328	4.9 ± 0.1	
	333	5.8 ± 0.1	
2-propanol	298.2	1.95	(Shakeel <i>et al.</i> , 2017)
	303.2	2.07	
	308.2	2.22	
	313.2	2.37	
	318.2	2.55	
	298.2	1.93	(Haq <i>et al.</i> , 2017)
	303.2	2.06	
	308.2	2.23	
	313.2	2.33	
	318.2	2.58	
ethyl acetate	298.2	1.30	(Shakeel <i>et al.</i> , 2017)
	303.2	1.43	
	308.2	1.59	
	313.2	1.76	
	318.2	1.98	

Table A.7 Solubility in mole fraction of ferulic acid in water.

Temperature (K)	Solubility $\times 10^5$ (mole fraction)	Reference
298.2	4.89	
303.2	6.25	
308.2	8.07	(Shakeel <i>et al.</i> , 2017)
313.2	10.9	
318.2	13.6	
293	4.6 ± 0.2	
298	4.9 ± 0.1	
303	6.2 ± 0.3	
308	7.9 ± 0.5	
313	11.3 ± 0.4	(Bitencourt <i>et al.</i> , 2016)
318	13.5 ± 0.2	
323	17.1 ± 0.3	
328	22.0 ± 0.4	
333	27 ± 1	
298.2	4.87	
303.2	6.22	
308.2	8.10	(Haq <i>et al.</i> , 2017)
313.2	11.1	
318.2	13.8	

Table A.8 Solubility in mol/kg of ferulic acid in water measured by Noubigh *et al.* (2007).

Temperature (K)	Solubility (mol/kg)
293.15	0.0215
298.15	0.0299
303.15	0.0371
308.15	0.0455
313.15	0.0551
318.15	0.0651

Table A.9 Solubility in g/L of ferulic acid in water measured by Mota *et al.* (2008).

Temperature (K)	Solubility (g/L)
288.15	0.57 ± 0.01
298.15	0.78 ± 0.01
303.15	0.92 ± 0.01
313.15	1.76 ± 0.02
323.15	2.19 ± 0.03

The following table presents the solubility data found in the literature for *trans*-cinnamic, *p*-coumaric and ferulic acids in solvents not studied in this work.

Table A.10 Solubility in mole fraction of cinnamic acids in solvents not studied in this work.

Compound	Solvent	Temperature (K)	Solubility (mole fraction)	Reference
<i>trans</i> -cinnamic acid	1-butanol	298.15	0.0691	(Li <i>et al.</i> , 2016)
		313.15	0.1015	
	isobutanol	298.15	0.0551	
<i>p</i> -coumaric acid	1-butanol	298.15	0.0371	(Ji <i>et al.</i> , 2016)
		313.15	0.0582	
	isobutanol	298.15	0.0226	
		313.15	0.0332	
	acetone	298.15	0.0428	
		313.15	0.0574	
		methyl acetate	298.15	
313.15	0.0292			
ferulic acid	ethylene glycol	298.15	0.0207	(Shakeel <i>et al.</i> , 2017)
		313.15	0.0252	
	1-butanol	298.15	0.0161	
		313.15	0.0213	
	2-butanol	298.15	0.0168	
		313.15	0.0220	
	DMSO	298.15	0.0526	
		313.15	0.0612	

Appendix B: NRTL-SAC Parameters from Literature

Table B.1 NRTL Binary parameters for conceptual segments in NRTL-SAC (Chen and Song, 2004).

segment 1	X	X	Y^-	Y^+	X
segment 2	Y^-	Z	Z	Z	Y^+
τ_{12}	1.643	6.547	-2.000	2.000	1.643
τ_{22}	1.834	10.949	1.787	1.787	1.834
$\alpha_{12} = \alpha_{22}$	0.2	0.2	0.3	0.3	0.2

Table B.2 NRTL-SAC molecular parameters for common solvents (Chen and Crafts, 2006).

Solvent name	X	Y^-	Y^+	Z
acetic acid	0.048	0.222	0.195	0.206
acetone	0.131	0.109	0.513	
acetonitrile	0.018	0.131	0.883	
anisole	0.536	0.01	0.653	
benzene	0.615		0.281	
1-butanol	0.425	0.004		0.49
2-butanol	0.343	0.069		0.393
n-butyl acetate	0.317	0.03	0.33	
methyl tert-butyl ether	0.483	0.105	0.142	
carbon tetrachloride	0.739	0.027	0.142	
chlorobenzene	0.727	0.024	0.484	
chloroform	0.393		0.167	
cumene	1.161			
cyclohexane	0.892			
1,2-dichloroethane	0.394		0.691	
1,1-dichloroethylene	0.529		0.208	
1,2-dichloroethylene	0.188		0.832	
dichloromethane	0.459		0.427	0.038
1,2-dimethoxyethane	0.277	0.03	0.077	0.057
N,N-dimethylacetamide	0.16	0.778	0.193	
N,N-dimethylformamide	0.18	0.752	0.254	
dimethyl sulfoxide		1.114		
1,4-dioxane	0.154	0.086	0.401	

Table B.2 (Continued).

Solvent name	X	Y ⁻	Y ⁺	Z
ethanol	0.251	0.03		0.63
2-ethoxyethanol	0.179	0.121	0.106	0.323
ethyl acetate	0.339	0.058	0.441	
ethylene glycol		0.343		0.852
diethyl ether	0.387	0.028	0.177	
ethyl formate	0.256	0.305		
formamide		0.089	0.341	0.252
formic acid		0.09		0.42
n-heptane	1.152			
n-hexane	1			
isobutyl acetate	0.62	0.183	0.541	
isopropyl acetate	0.552	0.154	0.498	
methanol	0.09	0.139		0.594
2-methoxyethanol	0.082	0.095	0.18	0.361
methyl acetate	0.239		0.338	
3-methyl-1-butanol	0.419		0.538	0.314
methyl butyl ketone	0.673	0.224	0.469	
methylcyclohexane	1.053		0.246	
methyl ethyl ketone	0.261	0.095	0.463	
methyl isobutyl ketone	0.673	0.224	0.469	
isobutanol	0.566		0.067	0.485
N-methyl-2-pyrrolidone	0.252	0.79	0.281	
nitromethane	0.122		1.032	0.051
n-pentane	0.898			
1-pentanol	0.458	0.024		0.491
1-propanol	0.374	0.013		0.53
isopropyl alcohol	0.332			0.636
n-propyl acetate	0.514	0.134	0.587	
pyridine	0.135		0.305	0.249
sulfolane	0.209	0.089		0.708
tetrahydrofuran	0.235	0.04	0.32	
1,2,3,4-tetrahydronaphthalene	0.924		0.865	

Table B.2 (Continued).

Solvent name	<i>X</i>	<i>Y</i>⁻	<i>Y</i>⁺	<i>Z</i>
toluene	0.604		0.304	
1,1,1-trichloroethane	0.548		0.287	
trichloroethylene	0.552		0.262	
m-xylene	0.758	0.021	0.316	
water				1
triethylamine	0.403	0.03		
1-octanol	0.867			0.534
N-octane	1.253			

Appendix C: Abraham's Solvation Model Coefficients from Literature

Table C.1 Coefficients in the linear free energy relationships (LFER) for water–solvent partitions as $\log P$ at 25 °C (Abraham *et al.*, 2015), considering dry solvents.

Solvent	<i>c</i>	<i>e</i>	<i>s</i>	<i>a</i>	<i>b</i>	<i>v</i>
methanol	0.276	0.334	− 0.714	0.243	− 3.320	3.549
ethanol	0.222	0.471	− 1.035	0.326	− 3.596	3.857
propan-1-ol	0.139	0.405	− 1.029	0.247	− 3.767	3.986
butan-1-ol	0.165	0.401	− 1.011	0.056	− 3.958	4.044
pentan-1-ol	0.15	0.536	− 1.229	0.141	− 3.864	4.077
hexan-1-ol	0.115	0.492	− 1.164	0.054	− 3.978	4.131
heptan-1-ol	0.035	0.398	− 1.063	0.002	− 4.342	4.317
octan-1-ol	− 0.034	0.489	− 1.044	− 0.024	− 4.235	4.218
decan-1-ol	− 0.058	0.616	− 1.319	0.026	− 4.153	4.279
propan-2-ol	0.099	0.344	− 1.049	0.406	− 3.827	4.033
iso-butanol	0.188	0.354	− 1.127	0.016	− 3.568	3.986
butan-2-ol	0.127	0.253	− 0.976	0.158	− 3.882	4.114
t-butanol	0.211	0.171	− 0.947	0.331	− 4.085	4.109
3-methylbutan-1-ol	0.073	0.36	− 1.273	0.09	− 3.770	4.273
pentan-2-ol	0.115	0.455	− 1.331	0.206	− 3.745	4.201
trifluoroethanol	0.395	− 0.094	− 0.594	− 1.280	− 1.274	3.088
ethylene glycol	− 0.270	0.578	− 0.511	0.715	− 2.619	2.729
diethyl ether	0.33	0.401	− 0.814	− 0.457	− 4.959	4.32
dibutylether	0.203	0.369	− 0.954	− 1.488	− 5.426	4.508
methyl t-butyl ether	0.376	0.264	− 0.788	− 1.078	− 5.030	4.41
tetrahydrofuran	0.207	0.372	− 0.392	− 0.236	− 4.934	4.447
dioxane	0.098	0.35	− 0.083	− 0.556	− 4.826	4.172
methyl acetate	0.351	0.223	− 0.150	− 1.035	− 4.527	3.972
ethyl acetate	0.328	0.369	− 0.446	− 0.700	− 4.904	4.15
propyl acetate	0.288	0.363	− 0.474	− 0.784	− 4.938	4.216
isopropyl acetate	0	0	0	0	0	0

Table C.1 (Continued).

Solvent	<i>c</i>	<i>e</i>	<i>s</i>	<i>a</i>	<i>b</i>	<i>v</i>
butyl acetate	0.248	0.356	-0.501	-0.867	-4.973	4.281
propanone	0.313	0.312	-0.121	-0.608	-4.753	3.942
butanone	0.246	0.256	-0.080	-0.767	-4.855	4.148
cyclohexanone	0.038	0.225	0.058	-0.976	-4.842	4.315
dimethylformamide	-0.305	-0.058	0.343	0.358	-4.865	4.486
dimethylacetamide	-0.271	0.084	0.209	0.915	-5.003	4.557
diethylacetamide	0.213	0.034	0.089	1.342	-5.084	4.088
dibutylformamide	0.332	0.302	-0.436	0.358	-4.902	3.952
N-methylpyrrolidinone	0.147	0.532	0.225	0.84	-4.794	3.674
N-methyl-2-piperidone	0.056	0.332	0.257	1.556	-5.035	3.983
N-formylmorpholine	-0.032	0.696	-0.062	0.014	-4.092	3.405
N-methylformamide	0.114	0.407	-0.287	0.542	-4.085	3.471
N-ethylformamide	0.22	0.034	-0.166	0.935	-4.589	3.73
N-methylacetamide	0.09	0.205	-0.172	1.305	-4.589	3.833
N-ethylacetamide	0.284	0.128	-0.442	1.18	-4.728	3.856
formamide	-0.171	0.07	0.308	0.589	-3.152	2.432
acetonitrile	0.413	0.077	0.326	-1.566	-4.391	3.364
nitromethane	0.023	-0.091	0.793	-1.463	-4.364	3.46
DMSO	-0.194	0.327	0.791	1.26	-4.540	3.361
tributylphosphate	0.327	0.57	-0.837	-1.069	-4.333	3.919

Appendix D: Calibration Curves by UV-Vis Spectroscopy

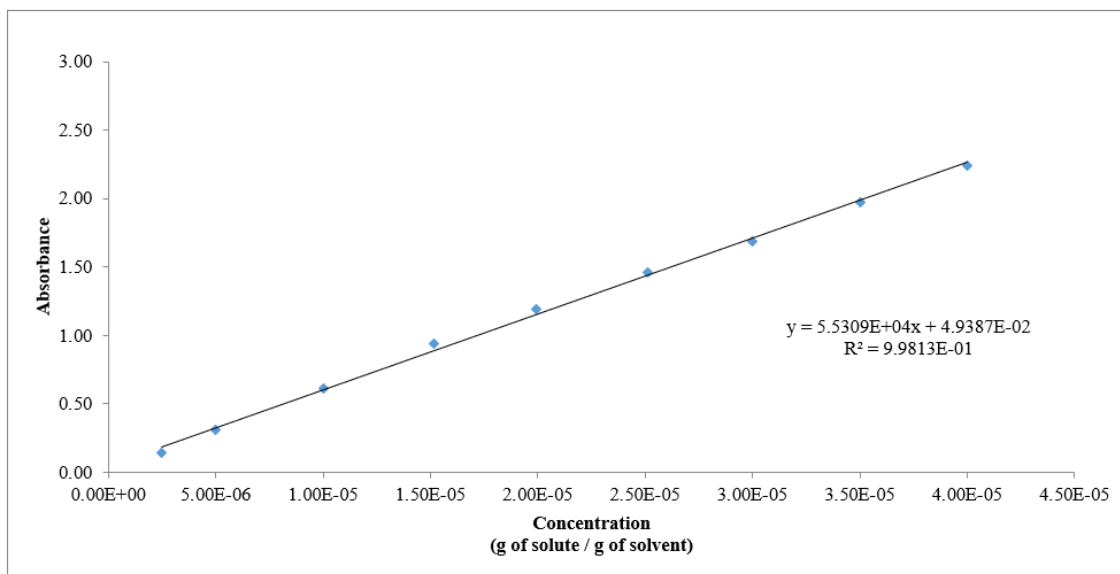


Figure D.1 Calibration curve of *trans*-cinnamic acid in water + ethanol (35:65, wt.%) mixed solvent, at 273 nm.

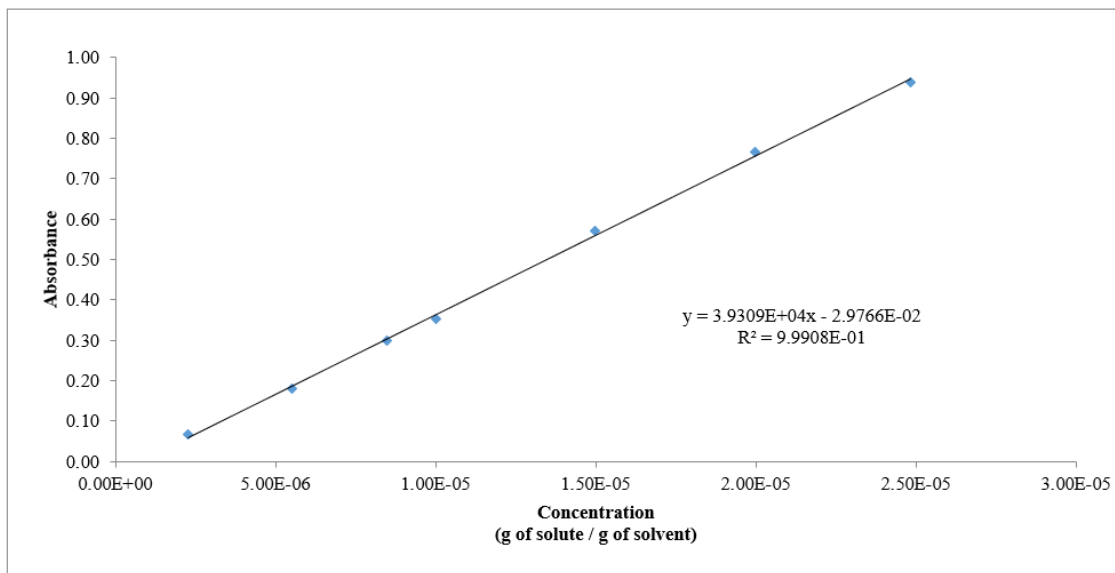


Figure D.2 Calibration curve of ferulic acid in water + ethanol (35:65, wt.%) mixed solvent, at 321 nm.

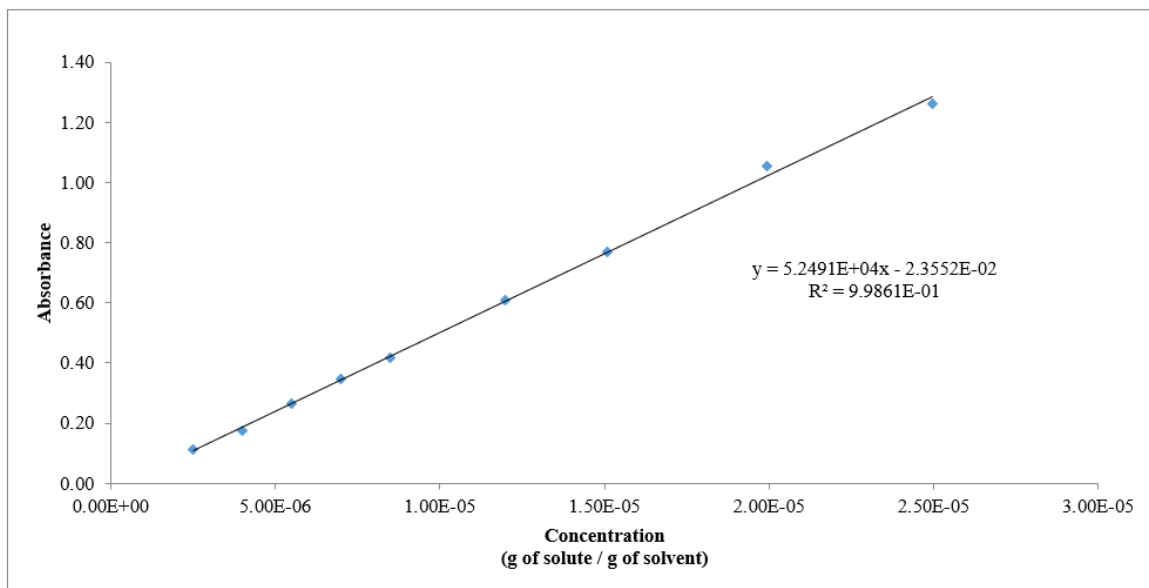


Figure D.3 Calibration curve of *p*-coumaric acid in water + ethanol (35:65, wt.%) mixed solvent, at 310 nm.

Appendix E: Results from Differential Scanning Calorimetry

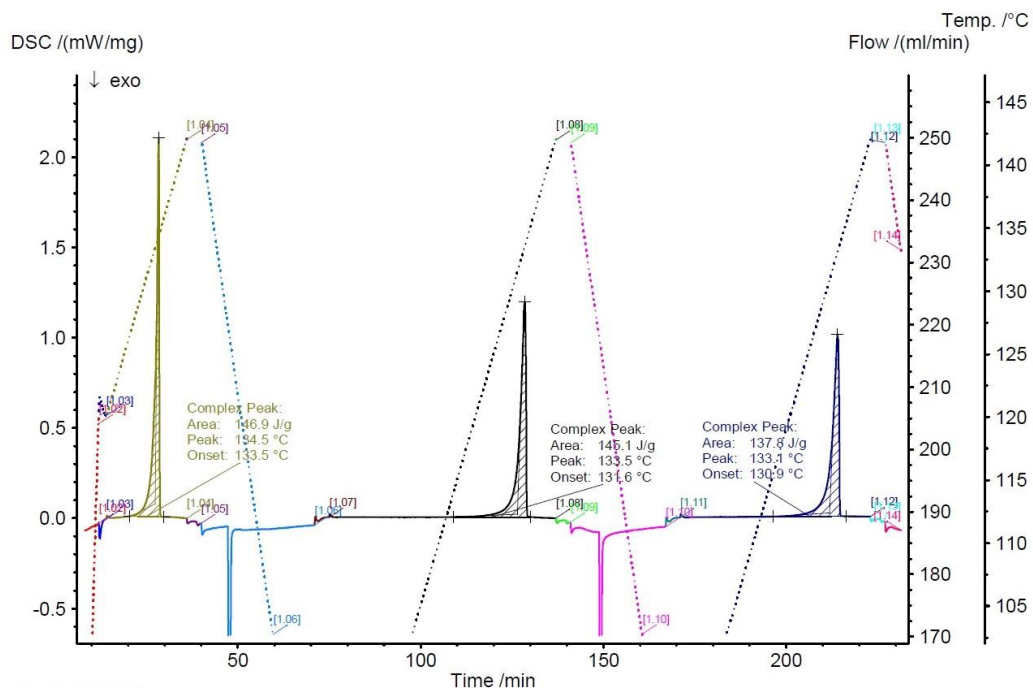


Figure E.1 Differential scanning calorimetry diagram of *trans*-cinnamic acid.

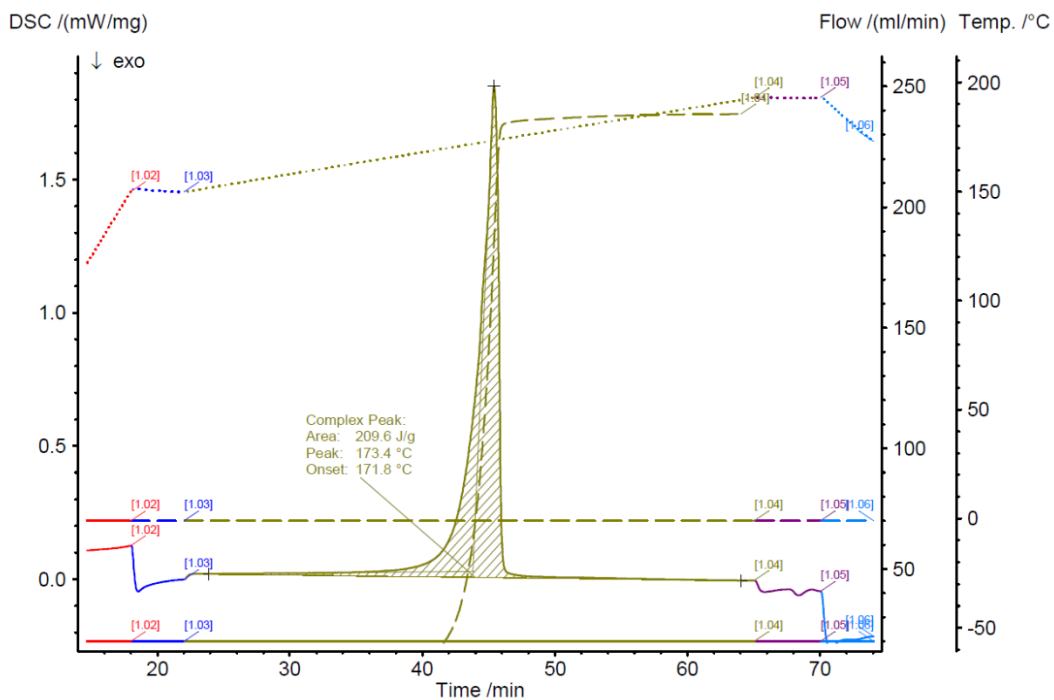


Figure E.2 Differential scanning calorimetry diagram of ferulic acid.

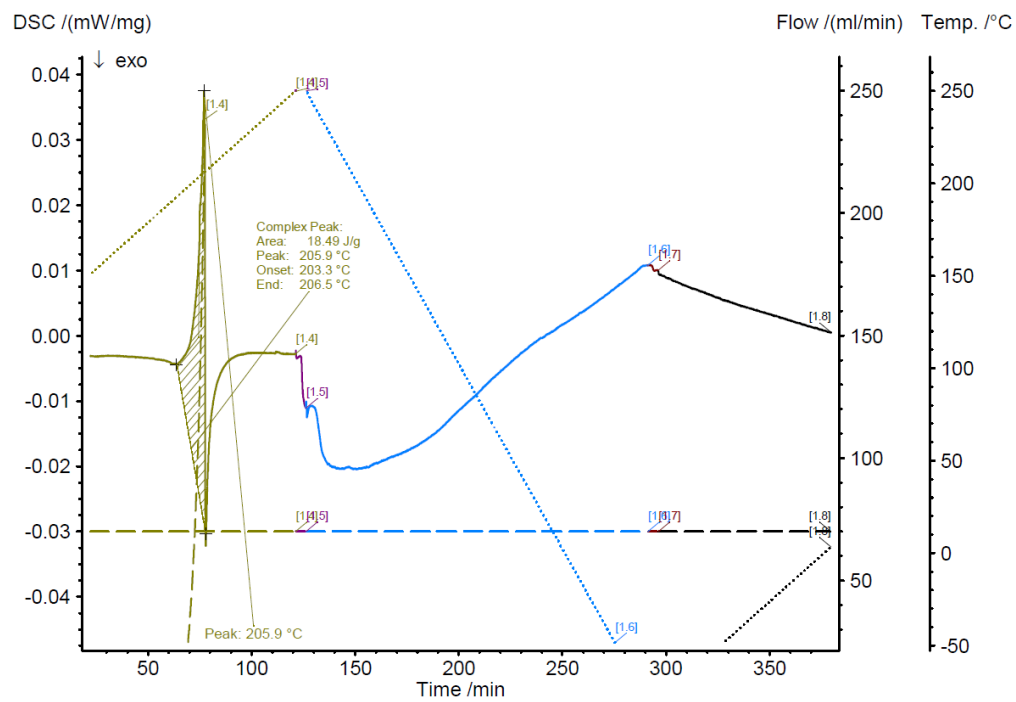


Figure E.3 Differential scanning calorimetry diagram of *p*-coumaric acid.